AD-A032 294 NAVAL POSTGRADUATE SCHOOL MONTEREY CALIF F/G 8/1
AN EVALUATION OF A COMPUTER SIMULATION MODEL OF PLANKTON DYNAMI--ETC(U)
SEP 76 D E HENRICKSON

UNCLASSIFIED NL

1 OF 1
ADA032294

END
DATE FILMED
1 -77

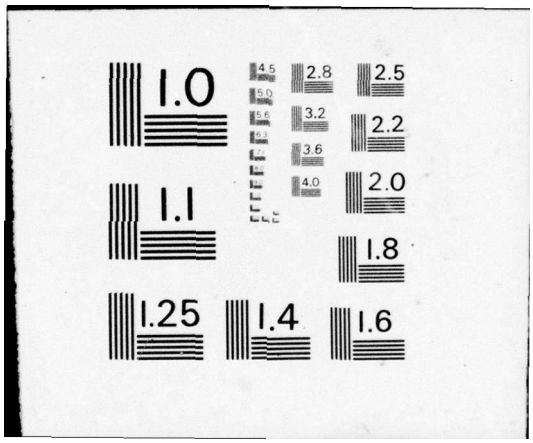
1.0
1.1
1.25
1.4
1.6
1.8
2.0
2.2
2.5
2.8
3.2
3.6
4.0
4.5
5.0
5.6

NAVAL POSTGRADUATE SCHOOL
Monterey, California

THESIS

AN EVALUATION OF A COMPUTER SIMULATION MODEL OF PLANKTON DYNAMICS IN MONTEREY BAY

by

David Edward Henrickson

September 1976

Thesis Advisor: E. D. Traganza

SECURITY CLASSIFICATION OF THIS PAGE (When Data Entered)

REPORT DOCUMENTATION PAGE		READ INSTRUCTIONS BEFORE COMPLETING FORM
1. REPORT NUMBER	2. GOVT ACCESSION NO.	3. RECIPIENT'S CATALOG NUMBER
4. TITLE (and Subtitle) (6) An Evaluation of a Computer Simulation Model of Plankton Dynamics in Monterey Bay.		5. TYPE OF REPORT & PERIOD COVERED Master's Thesis; September 1976
		6. PERFORMING ORG. REPORT NUMBER
7. AUTHOR(s) (10) David Edward Henrickson		8. CONTRACT OR GRANT NUMBER(s)
9. PERFORMING ORGANIZATION NAME AND ADDRESS Naval Postgraduate School Monterey, California 93940		10. PROGRAM ELEMENT, PROJECT, TASK AREA & WORK UNIT NUMBERS (12) 92p.
11. CONTROLLING OFFICE NAME AND ADDRESS (11) Naval Postgraduate School Monterey, California 93940		12. REPORT DATE September 1976
		13. NUMBER OF PAGES 93
14. MONITORING AGENCY NAME & ADDRESS (if different from Controlling Office) Naval Postgraduate School Monterey, California 93940		15. SECURITY CLASS. (of this report) Unclassified
		15a. DECLASSIFICATION/DOWNGRADING SCHEDULE

16. DISTRIBUTION STATEMENT (of this Report)

Approved for public release; distribution unlimited.

17. DISTRIBUTION STATEMENT (of the abstract entered in Block 20, if different from Report)

18. SUPPLEMENTARY NOTES

19. KEY WORDS (Continue on reverse side if necessary and identify by block number)

20. ABSTRACT (Continue on reverse side if necessary and identify by block number)

A computer simulation model of the phosphate, phytoplankton and zooplankton dynamics in Monterey Bay was examined and modified. The model is driven by four forcing functions expressed as annual cycles of upwelling velocity, incident solar radiation, mixed layer depth, and mixed layer temperature. An alternate upwelling index was developed based on the local wind field. A revised radiation index is employed

(cont on p. 2)

DD FORM 1 JAN 73 1473 (Page 1)

EDITION OF 1 NOV 68 IS OBSOLETE S/N 0102-014-6601

(cont fr p 1)

based on the generation of both advective fog and low stratus cloud cover common during upwelling on the California coast. Analysis of the model's response to sinking and advection of phytoplankton was examined. The importance of seasonal increases in predators was introduced as a controlling factor in the seasonal growth of zooplankton. The model is able to predict the seasonal trends of phosphate, phytoplankton, and zooplankton throughout the year.

4

An Evaluation of a Computer Simulation

Model of Plankton Dynamics in Monterey Bay

by

David Edward Henrickson
Lieutenant, United States Coast Guard
B.S., United States Coast Guard Academy, 1971

Submitted in partial fulfillment of the
requirements for the degree of

MASTER OF SCIENCE IN OCEANOGRAPHY

from the
NAVAL POSTGRADUATE SCHOOL
September 1976

Author David E Henrickson

Approved by: Eugene D. Traganza
Thesis Advisor

Alden B Chace / Glenn A Davis
Second Reader

Dale F. Leipper
Chairman, Department of Oceanography

Carl R Bentley
Academic Dean

ABSTRACT

A computer simulation model of the phosphate, phytoplankton and zooplankton dynamics in Monterey Bay was examined and modified. The model is driven by four forcing functions expressed as annual cycles of upwelling velocity, incident solar radiation, mixed layer depth, and mixed layer temperature. An alternate upwelling index was developed based on the local wind field. A revised radiation index is employed based on the generation of both advective fog and low stratus cloud cover common during upwelling on the California coast. Analysis of the model's response to sinking and advection of phytoplankton was examined. The importance of seasonal increases in predators was introduced as a controlling factor in the seasonal growth of zooplankton. The model is able to predict the seasonal trends of phosphate, phytoplankton, and zooplankton throughout the year.

TABLE OF CONTENTS

LIST OF FIGURES

Figure

ACKNOWLEDGEMENTS

The author wishes to thank Dr. Eugene D. Traganza for allowing the author to join in his research project: Investigation of Biochemical Relationships for Determining Concentration of Zooplankton Biomass and its Correlation with Chemical and Acoustical Properties of the Ocean. This project was supported by the Office of Naval Research, Code 482, Arlington, Virginia.

Sincere appreciation is extended to Dr. Glenn Jung and Dr. Alden Chace for their helpful comments and pertinent recommendations in reviewing this research.

The author wishes to thank Dr. Robert Renard and the meteorology staff of the Naval Postgraduate School for assistance with obtaining and reducing wind data.

Finally, the author's sincerest gratitude is felt for his wife, Nancy, whose personal sacrifices during the past nine months have made completion of this project possible.

I. INTRODUCTION

A. PURPOSE

In the interests of assessing the biomass of oceanic areas, various mathematical models have been designed to predict the dynamic response of ecosystems to change in the physical and chemical environment. Such models necessarily rely on accurate characterization of the forcing functions and accurate representation of the system with equations which are consistent with the specific region under study.

Recent attention paid to modeling systems in upwelling regions, Coastal Upwelling Ecosystems Analysis (CUEA), has brought about developments in both these areas. Adequate data of a physical and chemical nature is becoming available and significant progress in the refinement of governing equations is evident (Walsh, 1973).

The research presented here was aimed at creating a simulation model to describe the seasonal plankton dynamics in Monterey Bay, California, as known from the best available data. An existing simulation model (Pearson, 1975) was evaluated in an effort to make refinements and to judge the applicability of the time simulation technique to the Monterey region, characterized by seasonal upwelling.

B. MODELING PHILOSOPHY IN THE ECOLOGICAL CONTEXT

The merit of mathematically modeling systems of a purely physical nature in which parameters, initial conditions,

boundary conditions and the variable relationships are readily specified is unique. The value of current models of a biological nature requires some comment.

According to Odum (1971) there are a number of reasons behind constructing any mathematical model. Prediction of future states of the variables involved is an end in itself. Use of the prediction accuracy to focus data acquisition efforts or direct attention to deficiencies in concepts is likewise valid. If the model is real in the sense that it attempts to predict changes in the state variables based on a framework drawn from research in the real world, then failures may be useful in delineating weaknesses in the governing equations.

Construction of a "real" model is at best difficult. A perfect model of an ecosystem assumes that "all states and rates of change of the variables are known at all times" (Walsh, 1973). Given the vastness of complex interactions in even the simplest of biological systems, it may be stated that "no perfect representation of the real world exists except the real world itself" (Walsh, 1973).

It follows then that certain assumptions, logical statements and approximations of real dynamics are necessary to allow the model to operate. The resulting model may bear little correlation to the actual physical, chemical and biological situation at hand. Again, the argument for constructing the model must be considered. For purposes of prediction, a model which makes a logical statement relating

two state variables in the attempt to specify a relationship which may be unknown in part or in whole has merit. The fact that the logic of the model is a crude simplification is incidental if the prediction capability is proven.

All models can be characterized on the basis of realism, precision, and generality (Odum, 1971). It has been suggested that these three qualities are mutually exclusive in ecological models (Patten, 1971). A fourth category, simplicity, might be considered. Exacting detail, while lending to realism and precision often forces the model to be specific. Only when the model becomes an isomorph, i.e., a one-to-one correspondence to the real world, will generality be restored (Walsh, 1973).

The problems in creating a realistic model have been discussed briefly. The value of this type of model lies in research guidance. Where a specific question is asked of an ecological model, precision in prediction capability may be enhanced by sacrificing the other qualities. Such an approach might be taken in a fisheries model where a precise output for a limited region is desired (Odum, 1971). Simplicity and generality at the expense of both precision and realism may enhance understanding of broad ecological concepts.

The study presented herein was conducted with the idea of creating a model having good predictive capabilities for conditions occuring over a long span of time in a limited oceanic region.

C. DESCRIPTION OF THE MODEL

The original ecosystem model was developed by Pearson (1975) as part of continuing research into the correlation of zooplankton biomass with the chemical and acoustic properties of the ocean (Traganza, 1976). It is the intent of this research to identify areas of weakness in the model and make the appropriate changes to the equations and input parameters. These changes include a refinement of the upwelling index and radiation index as well as inclusion of advection, sinking and predation terms in the governing equations.

The modeling technique used is a time dependent simulation solved digitally on an IBM 360 computer using the IBM Continuous Simulation Modeling Program (CSMP-360). The dynamic equations are written in non-linear differential form and driven by four exogenous forcing functions expressed as annual cycles of upwelling velocity, mixed layer depth, mixed layer temperature, and incident solar radiation. The output consists of annual cycles of phosphate concentration (microgram-atoms of phosphorous per liter, μg-atP/ℓ), phytoplankton biomass (grams of carbon per square meter, gC/m^2) and standing stock of herbivorous zooplankton (g C/m^2) in the mixed layer.

The Pearson version (Figure 1) of the model is defined by the following basic equations:

1) $$\frac{dX1}{dt} = NUT + REGEN - UPTAK \qquad (1)$$

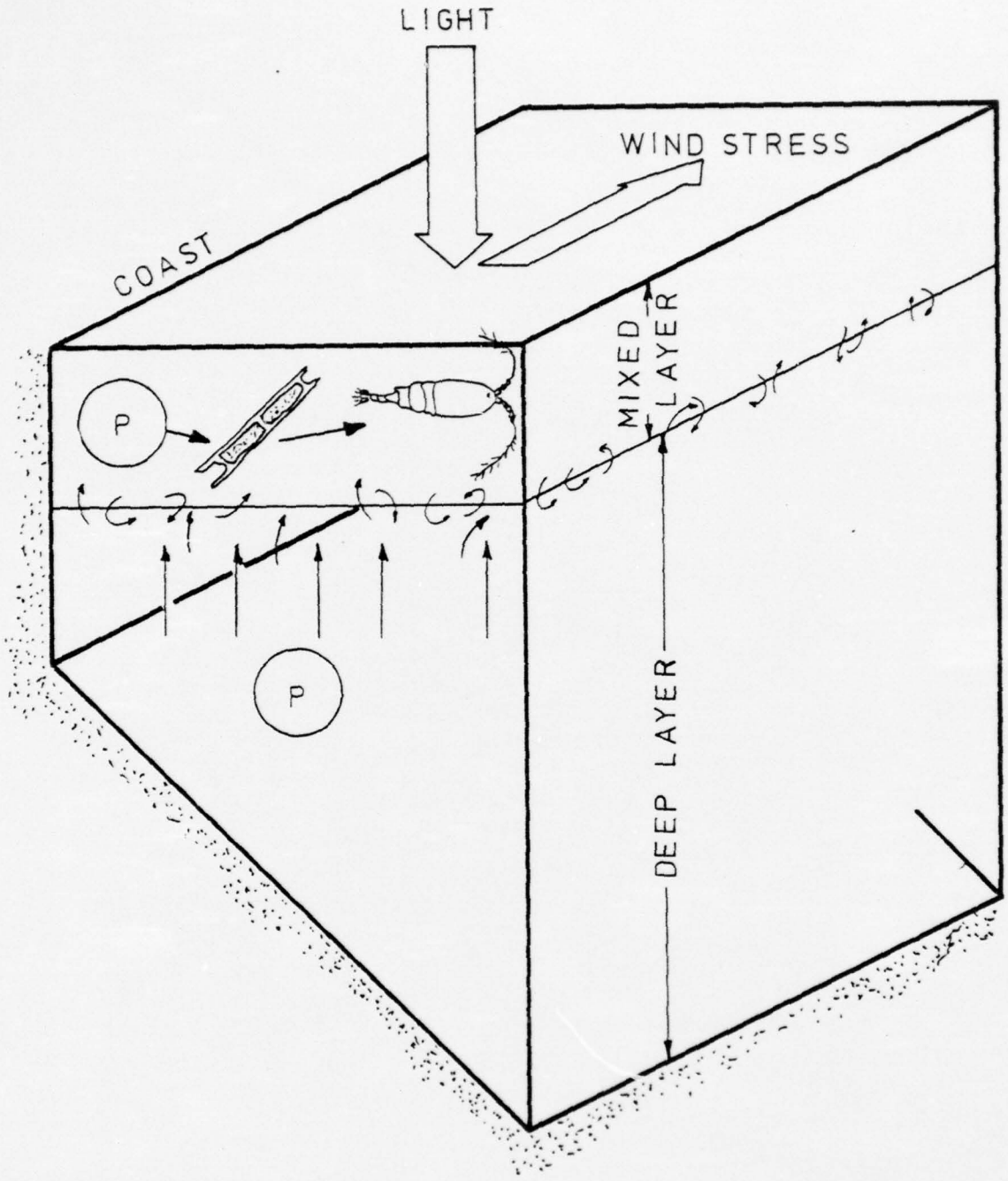

Figure 1. Pictoral representation of Monterey Upwelling Ecosystem.

where: $\frac{dX1}{dt}$ = time rate of change of phosphate concentration (µg-at P/l) in the mixed layer

NUT = input of phosphate from upwelling and mixing from below the mixed layer (µg-at P/l)

REGEN = phosphate recycled as biological excretory products within the mixed layer (µg-at P/l)

UPTAK = phosphate depleted by phytoplankton utilization (µg-at P/l)

2) $\frac{dX2}{dt}$ = PROD - RESP2 - GRAZ (2)

where: $\frac{dX2}{dt}$ = time rate of change of phytoplankton biomass (gC/m^2)

PROD = photosynthetic production (gC/m^2)

RESP2 = respiration losses (gC/m^2)

GRAZ = grazing losses (gC/m^2)

3) $\frac{dX3}{dt}$ = GRAZ - RESP3 - VOID - LOSS (3)

GRAZ = input due to ingestion of phytoplankton (gC/m^2)

RESP3 = respiration losses (gC/m^2)

VOID = excretory losses (gC/m^2)

LOSS = stock depletion by mortality (gC/m^2)

(Pearson, 1975)

II. BACKGROUND THEORY

A. UPWELLING THEORY

1. Ekman Dynamics

Seasonal upwelling of nutrient-rich deep water into the productive mixed layer is an important aspect of the Monterey Bay ecosystem. The principal source of phosphate in the mixed layer is vertical advection which is produced in response to wind-induced Ekman circulation. Theoretical calculations of the offshore component of horizontal current are based on Ekman pure drift theory in an infinitely deep, homogeneous ocean (Neumann and Pierson, 1966). The components of the horizontal current take the form:

$$U = V_o\, e^{-(\pi/D)Z}\, \mathrm{COS}[45-(\pi/D)Z] \quad \text{and} \tag{4a}$$

$$V = V_o\, e^{-(\pi/D)Z}\, \mathrm{SIN}[45-(\pi/D)Z] \tag{4b}$$

$$D = (A/\rho\omega\ \mathrm{SIN}\ \phi)^{\frac{1}{2}} \quad \text{and} \tag{5a}$$

$$V_o = \tau_y/Aa \tag{5b}$$

where:

U = velocity component in the x direction

V = velocity component in the y direction (parallel to wind)

V_o = surface velocity component (45^o to right of wind, Northern Hemisphere)

Z = depth

D = Ekman depth of frictional resistance

A = coefficient of eddy viscosity

τ_y = surface wind stress in y direction (dynes)

a = $f\rho/A$

ϕ = latitude

ρ = density of water (g/cm^3)

f = Coriolis parameter = 2ω SIN ϕ

The coefficient of eddy viscosity, A, was assumed constant since detailed information on the small scale motions of the surface layer was not available. This assumption is generally made in mass transport studies (Neumann, 1968).

The mass transport due to wind driven current is found by integrating the equations of velocity (U and V) over the depth of the water column, as shown:

$$S_x = \rho \int UdZ = \tau_y/f \qquad (6a)$$

and

$$S_y = \rho \int VdZ = 0 \qquad (6b)$$

where:

S_x = mass transport in the x direction

S_y = mass transport in the y direction

From the equations for mass transport, it is observed that the net transport is 90 degrees to the right of the wind in the northern hemisphere and that it is directly proportional to the wind stress acting on the sea surface, parallel to the coast.

2. Wind Stress on the Sea Surface

The coupling of wind energy to the water at the air-sea interface is defined by the conventionally-accepted form of the wind stress equation:

$$T_y = \rho' C_z W_z^2 \qquad \text{(Gordon, 1972)} \qquad (7)$$

where: T_y = wind stress parallel to the coast (dynes/cm^2)

ρ' = density of air

C_z = drag coefficient at height z (non-dimensional)

W_z = wind speed at height z (cm/sec)

As in other momentum exchange studies, the dynamic coefficients appear to present the singular most difficult problem. Wilson (1960) states that the drag coefficient for air flow over a water surface is dependent on the wind speed (W), the height of measurement(z), a surface roughness parameter (z_o), and atmospheric stability terms. There may be additional dependence on oceanic parameters of depth, fetch distance and wave height. An average value of the drag coefficient for high wind speeds (i.e. greater than 10 m/sec) of 2.37×10^{-3} is arrived at by examination of research completed through 1959 (Wilson, 1960).

Work by Deacon (1962) established an empirical relationship for winds up to 13 meters/second which gives a linear dependence of C_z (at z = 10m) to the wind speed as follows:

$$C_{10} = (1.10 + 0.04\, W_{10}) \times 10^{-3} \text{ for W in m/sec} \qquad (8)$$

(Roll, 1965)

Deacon's research was carried out using data from ship observations and coastal regions.

3. Spatial Extent

The offshore movement of water in a region bounded by a coastline causes replacement water to be upwelled from below the layer affected by the surface wind stress. Accordingly, it is necessary to specify the spatial dimensions of the region in order to apply principles of continuity in determining the vertical current speed. The significant parameters involved in upwelling are: (1) the offshore horizontal dimension of the upwelling region, which is most directly related to the width of the wind field; (2) the offshore component of the Ekman current (U); and (3) the depth of the Ekman layer (D).

Estimates of the maximum depth of the source of upwelled water in a coastal region are approximately 100 to 200 meters (Neuman and Pierson, 1966) based on the slope of the isotherms. The mass transport offshore due to wind drift current has been previously detailed as occurring in a surface layer of depth, D, corresponding to the Ekman depth of frictional resistance; regardless of the source depth of the upwelled water, it transgresses the "boundary" at depth, D, before being carried offshore. The vertical dimension of the region is then readily specified. It is assumed that the depth of frictional resistance (D) and the depth of the mixed layer (Z) are approximately coincident. The differences between (D) and (Z) are important when phytoplankton

are advected out of the Ekman layer but exist throughout the mixed layer.

The horizontal extent of the upwelling region is considerably more nebulous than the depth of the mixed layer. Classical estimates of this dimension limit the zone to probably no more than 100 kilometers in offshore width. It may be expected that the width of the region is dependent on several factors; among them, the width of the wind field, variations and non-linearities in the energy exchange processes due to surface roughness characteristics or stability changes in both the atmosphere and the water column, as well as spatial and temporal oscillations of the significant wind vector. In addition, local coastal and bottom topography may figure extensively in the problem as will be discussed later.

Sverdrup (1938) observed a relatively well defined offshore boundary to a coastal upwelling zone, coincident witha downwind current which was marked by an intense vertical gradient of velocity (Sverdrup et al., 1942). He further observed an offshore migration of the current band at a rate somewhat less than the speed of the offshore surface current within the upwelling region. The latter fact implied the possibility of cellular circulation patterns in the near surface upwelling zone.

Hidaka (1954) proposed a steady state theory of upwelling in which he defined a horizontal frictional distance, D_h, analogous to the depth of frictional resistance

appearing in Ekman's work. Applying reasonable values to Hidaka's expression confines the total cellular circulation region to a width of about 15 kilometers. The width of the region is defined by:

$$D_H = \pi(2A_H/2\omega \text{ SIN } \phi)^{\frac{1}{2}} \text{ where: } A_H = 10^7 (gcm^{-1} \text{ sec}^{-1}) \quad (9)$$

(Smith, 1968)

Downward vertical currents occurring in the seaward half of the cell limit the upwelling to a width of 7.5 kilometers. The theoretical width is not consistent with observations of upwelling at greater distances from the coast (Barnes, 1969).

Yoshida (1967) developed a quasi-steady state model applicable to eastern boundary current regions (Smith, 1968). An expression was derived for the horizontal dimension of the coastal upwelling region which is given by:

$$L_x = \frac{(gH\Delta\rho/\rho)^{\frac{1}{2}}}{f} (H\mu/D\gamma)^{\frac{1}{2}} \text{ for latitudes greater than 22 degrees} \quad (10)$$

where: L_x = horizontal width of the coastal boundary region (m)

g = gravitational acceleration ($m\text{-}sec^{-2}$)

H = thickness of the upper layer (m)

D = H + thickness of the lower layer (m)

f = Coriolis parameter (sec^{-1})

ρ = density of water ($g\text{-}cm^{-3}$)

$\Delta\rho$ = density difference between deep and surface layers ($g\text{-}cm^{-3}$)

μ = internal friction coefficient (sec^{-1})

γ = 2×10^{-7} sec^{-1} (Smith, 1968)

B. CURRENTLY AVAILABLE UPWELLING INDEX

Bakun (1976) has calculated coastal upwelling indices for the coast of North America using Fleet Numerical Weather Central monthly mean pressure fields to compute the geostrophic wind. Analysis is done on a 63 x 63 point grid of approximately 200 nautical mile mesh length (Bakun, 1973). Figure 2 shows Bakun's results for 1974 at 36 degrees North, 122 degrees West, approximatley 50 miles south of Monterey Bay. In reviewing several aspects of hydrographic surveys taken in Monterey Bay, it was suspected that this region is characterized by local upwelling patterns not appearing in the index computed by Bakun. Further discussion follows in the methods section.

C. EFFECTS OF UPWELLING ON INCIDENT RADIATION

Cold water upwelled from depth during the spring and summer months brings about both advection fog and stratus cloud formation. The fog occurs as warm surface air is cooled by the cold seawater to its saturation point causing the condensation of the contained water vapor. Stratus clouds occur below the base of a quasi-permanent atmospheric temperature inversion (Tont, 1975).

The net effect of both fog and stratus layers is to reduce the amount of solar radiation reaching the sea surface during the upwelling period. Tont (1975) obtained mean values of solar radiation at the surface over the period 1950-1973 at San Diego. A correlation study of the annual upwelling index and the amount of sunlight at the surface

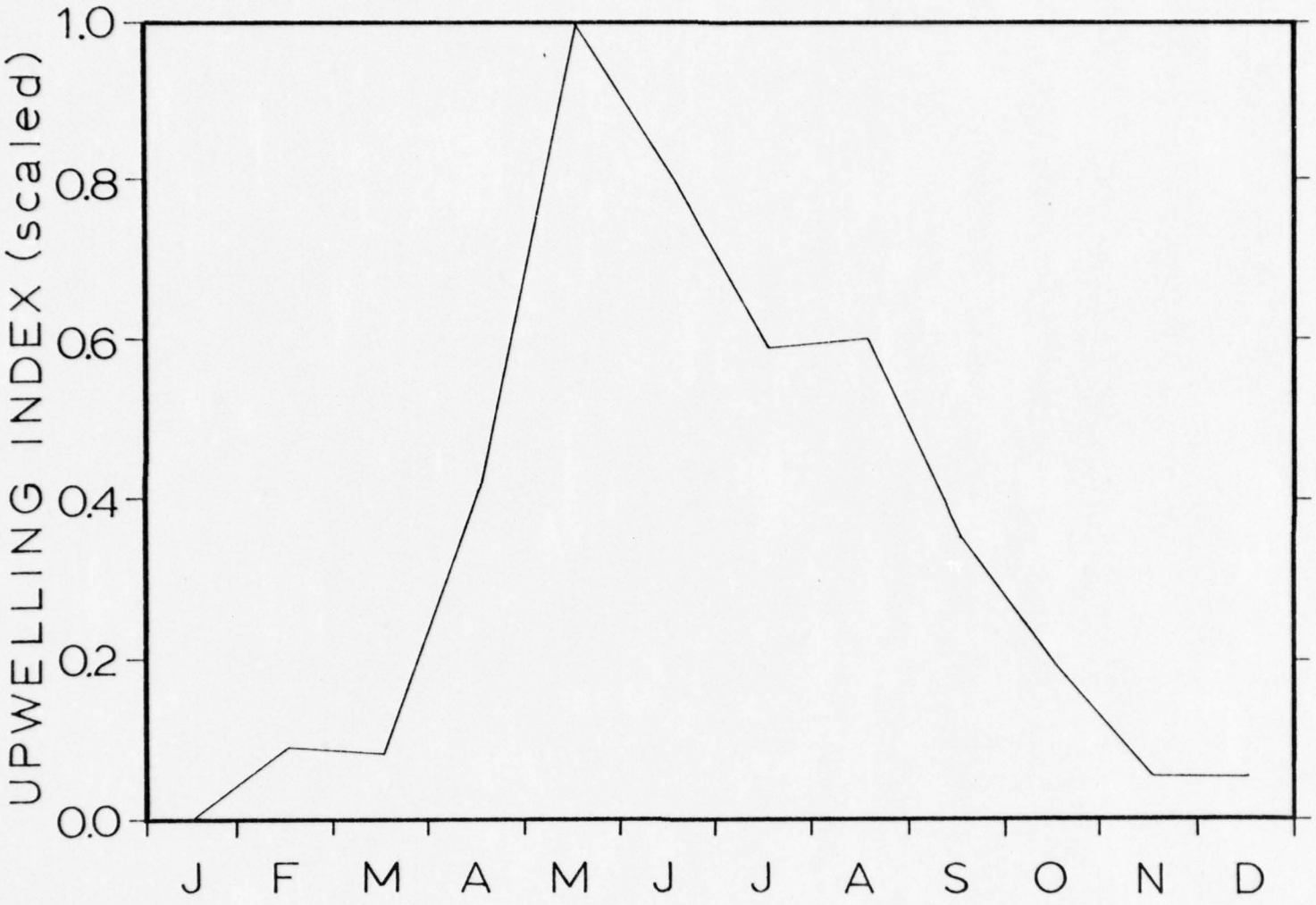

Figure 2. Upwelling index for 1974 at 36 degrees North, 122 degrees West, computed by Bakun.

showed a maximum of about 40 per cent reduction in available sunlight during the peak upwelling months. The result of Tont's research is shown in Figure 3.

D. SINKING OF ALGAL CELLS

Review of sedimentation rates of algal cells indicate justification for including a sinking term in the phytoplankton equation. The Pearson (1975) model assumes uniform algal concentation within the mixed layer. It is reasonable that changes in the concentration of phytoplankton caused by vertical movement out of the layer will occur.

Parsons and Takahashi (1973) state that the theoretical sinking rate of phytoplankton can be determined from:

$$V = \frac{2gr^2}{9} \left(\frac{\rho' - \rho}{\eta \cdot \phi_r}\right) \qquad (11)$$

where:

r = radius of the cell

g = gravitational acceleration

ρ' = density of the organism

ρ = density of the medium (sea water)

η = viscosity of the medium

ϕ_r = form resistance coefficient (accounts for non-spherical shapes)

Measured rates of sinking for live algal cells vary between zero and 30 meters per day according to Parsons and Takahashi (1973). These rates represent a broad range of species and sizes.

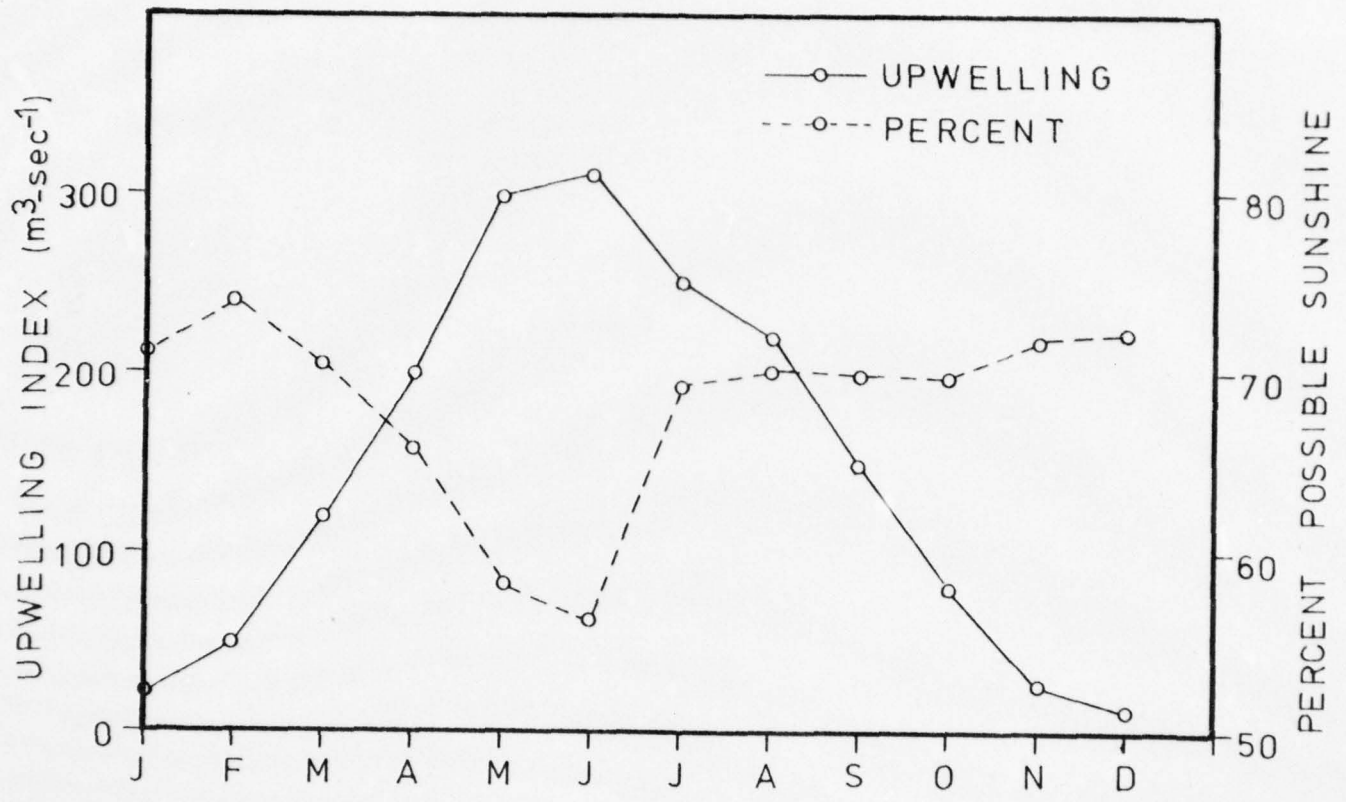

Figure 3. Monthly means of upwelling index (m^3/sec) and percent of possible sunshine (after Tont, 1975).

E. ADVECTION

It is known that significant current velocities occur within the mixed layer from Ekman dynamics. It might be expected then that the concentration of phosphate, phytoplankton and zooplankton will be affected by advection. O'Brien and Wrobleski (1972) have shown by scale analysis that advection and biological productivity of the Peru upwelling ecosystem are equally important.

The advective terms of the material derivative of a property (C) are written:

$$\text{Advective change} = U \frac{\partial C}{\partial X} + V \frac{\partial C}{\partial Y} + W \frac{\partial C}{\partial Z} \qquad (12)$$

where: U,V,W = velocity components in x, y, and z directions respectively

$\frac{\partial C}{\partial X}, \frac{\partial C}{\partial Y}, \frac{\partial C}{\partial Z}$ = gradients of the concentration of property (C) in the x, y, and z directions

A review of California Cooperative Fisheries Investigation (CALCOFI) data for 1974 (CALCOFI, 1974) shows that the phosphate concentration varies significantly in the vertical direction but the horizontal variation is not as significant.

It is assumed for the purposes of this model that the advection term for phosphate reduces to the vertical component:

$$\text{Advective change} = W \frac{\partial X1}{\partial Z} \qquad (13)$$

since: $\frac{\partial X1}{\partial X} = \frac{\partial X1}{\partial Y} = 0$

Pearson (1975) has included this term in the computer model as:

$$UPWELL = W \frac{DX1 - X1}{EKL} \qquad (14)$$

where:

W = vertical speed (m/day)

EKL = depth of the Ekman layer (m), EKL = D

DX1 = concentration of phosphate below the mixed layer (µg-at P/l)

X1 = concentration of phosphate in the mixed layer (constant) (µg-at P/l)

$\frac{DX1 - X1}{EKL}$ = vertical gradient of phosphate (µg-at P/m l)

The advection of zooplankton in the revised model is discounted because it is assumed that they have developed mechanisms which permit them to remain in a particular oceanic region by swimming or riding cellular circulation currents.

Phytoplankton, however, are affected by advection. CALCOFI data (CALCOFI, 1974) shows that the significant gradients of phytoplankton occur in the vertical and offshore directions; therefore, the advection expression for phytoplankton is reduced to:

$$\text{Advective change} = U \frac{\partial X2}{\partial X} + W \frac{\partial X2}{\partial Z} \qquad (15)$$

The horizontal velocity is related to the vertical velocity by continuity (when it is assumed that $\frac{dV}{dY} = 0$, parallel to the coast) such that:

$$U = - WL/D \qquad (16)$$

where: U = horizontal velocity component offshore (m/day)

W = upward vertical velocity component (m/day)

L = width of the region (m)

D = Ekman depth (m)

The phytoplankton advection term can be written:

$$\text{Advective change} = W\left[-\frac{L}{D}\frac{\partial X2}{\partial X} + \frac{\partial X2}{\partial Z}\right] \qquad (17)$$

The gradients of phytoplankton can be approximated by:

$$\frac{\partial X2}{\partial X} = \underset{\Delta X \to 0}{\text{LIM}}\ \frac{\Delta X2}{\Delta X} \quad \text{and} \quad \frac{\partial X2}{\partial Z} = \underset{\Delta Z \to 0}{\text{LIM}}\ \frac{\Delta X2}{\Delta Z} \qquad (18a\&b)$$

If it is assumed that the concentrations of phytoplankton below the mixed layer and outside the modeled area are much less than the concentration in the modeled region, then the gradient can be approximated by:

$$\frac{X2-0}{\Delta X} = \text{horizontal gradient;} \qquad (19)$$

$$\frac{X2-0}{\Delta Z} = \text{vertical gradient;} \qquad (20)$$

where: X2 = phytoplankton concentration in the mixed layer

ΔX = horizontal distance at which the concentration of phytoplankton becomes negligible with respect to the modeled area

ΔZ = vertical distance at which phytoplankton concentration becomes negligibly small

The phytoplankton advection term can then be written as:

$$\text{Advective change to Phytoplankton in the modeled area} = W(X2)\left[-\frac{L}{D\Delta X} + \frac{1}{\Delta Z}\right] \qquad (21)$$

The sign convention is established as positive (+) into the model area and negative (-) out.

F. PREDATION PRESSURE

Under constant environmental conditions, the dynamics of zooplankton growth are a function of the food supply and predation pressure. Natural processes of population control insure that a given species will not be eliminated by low food supply and high predation pressure or that unstable growth will not result from the inverse situation. Attempts to translate the stabilizing factors into mathematical terms often result in simplified general relationships that do not exhibit the flexibilities inherent in the real system. Notwithstanding the limitations, a predation term is included in the simulation model.

The long term survivability of both predator and prey is keyed directly to maintenance of a balance in energy expenditures and gains. To date, laboratory experiments to duplicate this balance have not been entirely successful. Prey stocks in small laboratory environments have been artificially supported by providing refuge where predator access to the prey was denied and by introducing additional prey to the system to replenish the supply (Patten, 1971). Nevertheless, population control by predation is prey-density dependent as a first approximation. For a system of one prey species and a single predator species, predation pressure may be represented by:

$$P = k_1 D \quad \text{for } 0<D<d_1 \text{ and}$$
$$P = k_2 \quad \text{for } D>d_1 \qquad (22)$$

where: P = predation pressure or food intake per unit predator

D = prey density

d_1 = satiation threshold of prey density

k_1 and k_2 = constants

Above prey density values of d_1, predator satiation will occur and pressure will level off at some constant high value. The function is shown on an arbitrary scale in Figure 4 according to Patten (1971). This simple relationship is not entirely satisfactory for the predator since low food supplies would result in starvation. Under such circumstances, and given a second prey species of perhaps less palatability, the predator would switch food intake to the more abundant species of prey. There are several obvious implications to the switching phenomenon:

1. predation on the most abundant species assures stable growth of that species,
2. switching from a declining species serves to prevent elimination of that species (Patten, 1971), and
3. elimination of the predator by overgrazing one available food source is avoided.

The model under consideration in this thesis is a single species approximation in which predation pressure is incorporated with other zooplankton mortality factors, i.e. morphological death, in the "LOSS" term. This term is given by Pearson (1975) as:

$$LOSS = L\ (X3) \qquad (23)$$

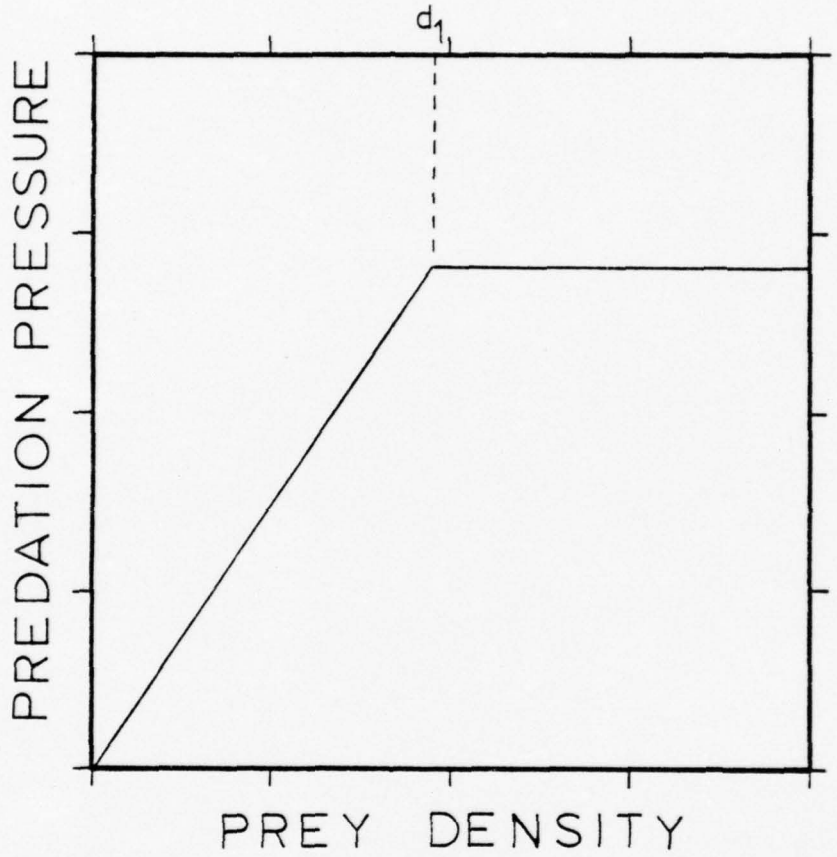

Figure 4. Predation pressure as a function of prey density (zooplankton biomass) (after Patten, 1971).

where: LOSS = fraction of the zooplankton population removed from the system in a day's time ($g\ C/m^2$ day)

L = constant rate of loss or percent loss per day (day^{-1})

X3 = zooplankton "standing crop" ($g\ C/m^2$)

Harriston concluded in 1960 that "herbivores are predator limited" (Patten, 1971).

Conclusions by Patten (1971) show that herbivores are both food and predator limited. Therefore, in the modified model, the LOSS term is reserved for variable predator limitation of herbivorous zooplankton and natural death of zooplankton herbivores is assumed to be negligible.

III. METHODS

The existing model appears weak in several areas. Originally, the forcing functions of upwelling and solar radiation which are critical to the simulation were obtained from average cycles for the California coast (upwelling) and the latitude band between 30 and 40 degrees north. Phytoplankton sinking and advection terms were lacking and the predation pressure term in the zooplankton equation needed improvement.

A. UPWELLING PROGRAM

A computer program was written to calculate the annual upwelling index for Monterey Bay. Wind data was obtained from the Monterey Peninsula Airport observations during 1974. Hourly observations were examined to determine the significant mean daily wind vector for each day and corrections were applied to speed and direction when indicated by topographic obstructions. Fortunately, no corrections were needed to northerly winds which are the driving mechanism for upwelling.

An x-y coordinate system was established such that the surface wind stress ($\tau_y = \rho' C W^2$) could be directly calculated from the wind component parallel to the coast. The Ekman mass transport (S_x), surface current velocity (V_o) and the average velocity within the Ekman layer (U) were calculated by the following relations:

$$V_o = \tau_y / Aa \qquad (5b)$$

where: V_o = surface current vector

and

$$\bar{U} = \frac{1}{D}\int_{o}^{Z} UdZ \qquad (24)$$

where: $\bar{U}$ = average velocity in x direction in the layer

and:

$$S_x = \tau_y/f \qquad (6a)$$

where S_x = mass transport in x direction (offshore)

The vertical current representing upwelling is determined per unit y (along coast) from the continuity equation, $(\nabla \cdot \hat{v}) = 0$, such that

$$\bar{U}(D) = W(L) \qquad (25)$$

where: $\bar{U}$ = average horizontal velocity in the Ekman layer (m/day)

W = upwelling speed (m/day)

D = Ekman depth (m)

L = horizontal width of the upwelling region (m)

Zero current is assumed parallel to the coast.

The horizontal width of the upwelling region, (L) was determined from Yoshida's (1967) equation. Applying typical values to this equation yields a horizontal width of 3 X 10^4 m.

Principles of continuity were used to arrive at the mean daily upwelling current values and these figures were averaged over a 30-day period.

B. RADIATION INDEX

A revised incident solar radiation index which takes into account the reduction of sunlight by local fog and stratus cloud cover was developed. Correlation of the measurements of surface irradiance and the strength of upwelling (as indicated by the upwelling index) by Tont (1975) is represented by Figure 5. This figure is derived from the results of Tont's study as shown in Figure 3 by plotting the percent of possible sunshine (Y-axis) as a function of the upwelling index (X-axis) which has been scaled to a maximum value of one. The resulting curves (A) and (B) show the conditions occurring after, and prior to, the upwelling maximum, respectively.

The difference exhibited between the curves may be due to changes in the character of the air mass brought about by seasonal migrations of the quasi-permanent thermal low over Nevada and the North Pacific sub-tropical high located west of the coast.

Figure 5 was used to calculate a revised incident radiation index by entering with the newly-developed upwelling index values and by applying the corresponding percent to the theoretical mean monthly radiation for clear sky conditions (possible sunlight). Figure 6 shows the possible sunlight throughout the year (from Tont, 1975) as Q_o, and the theoretical radiation at the surface (Q_i) after the effects of fog and clouds are considered.

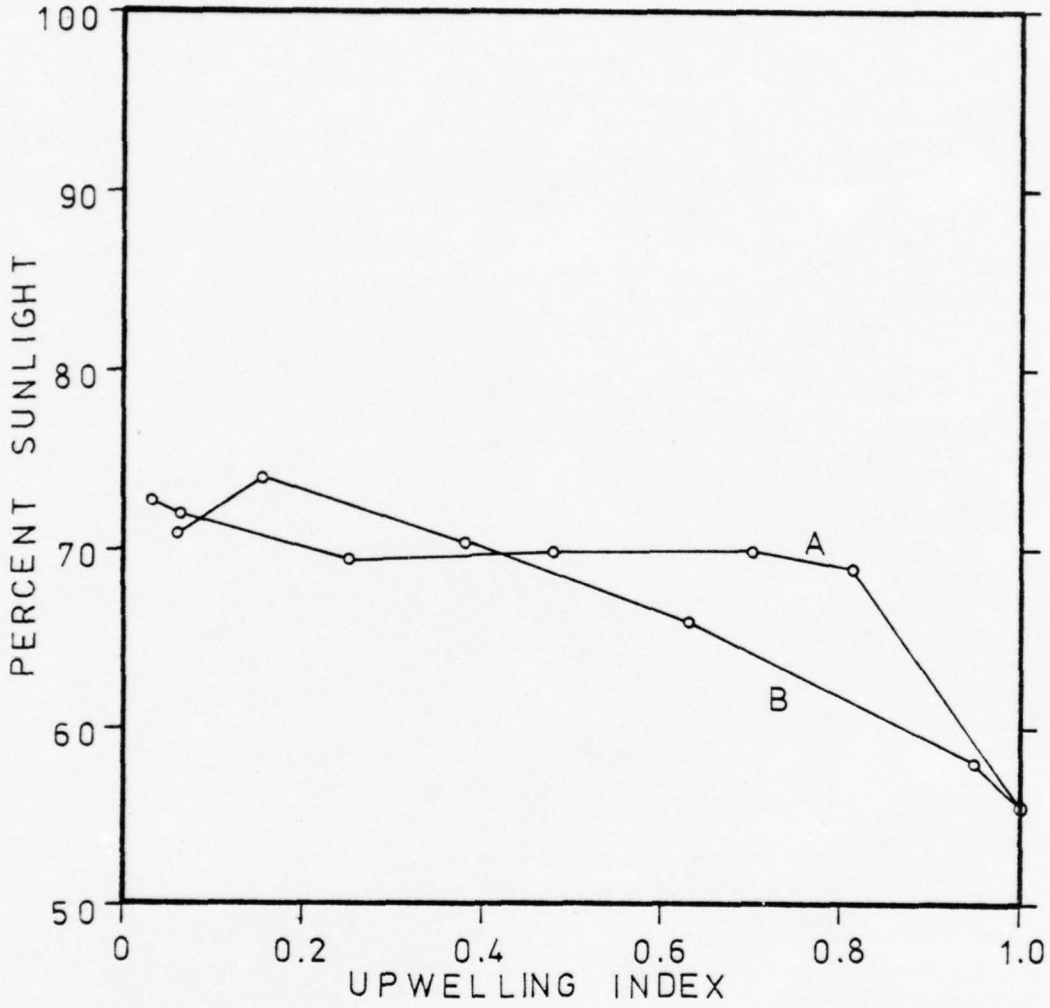

Figure 5. Percent of possible sunlight as a function of upwelling index.

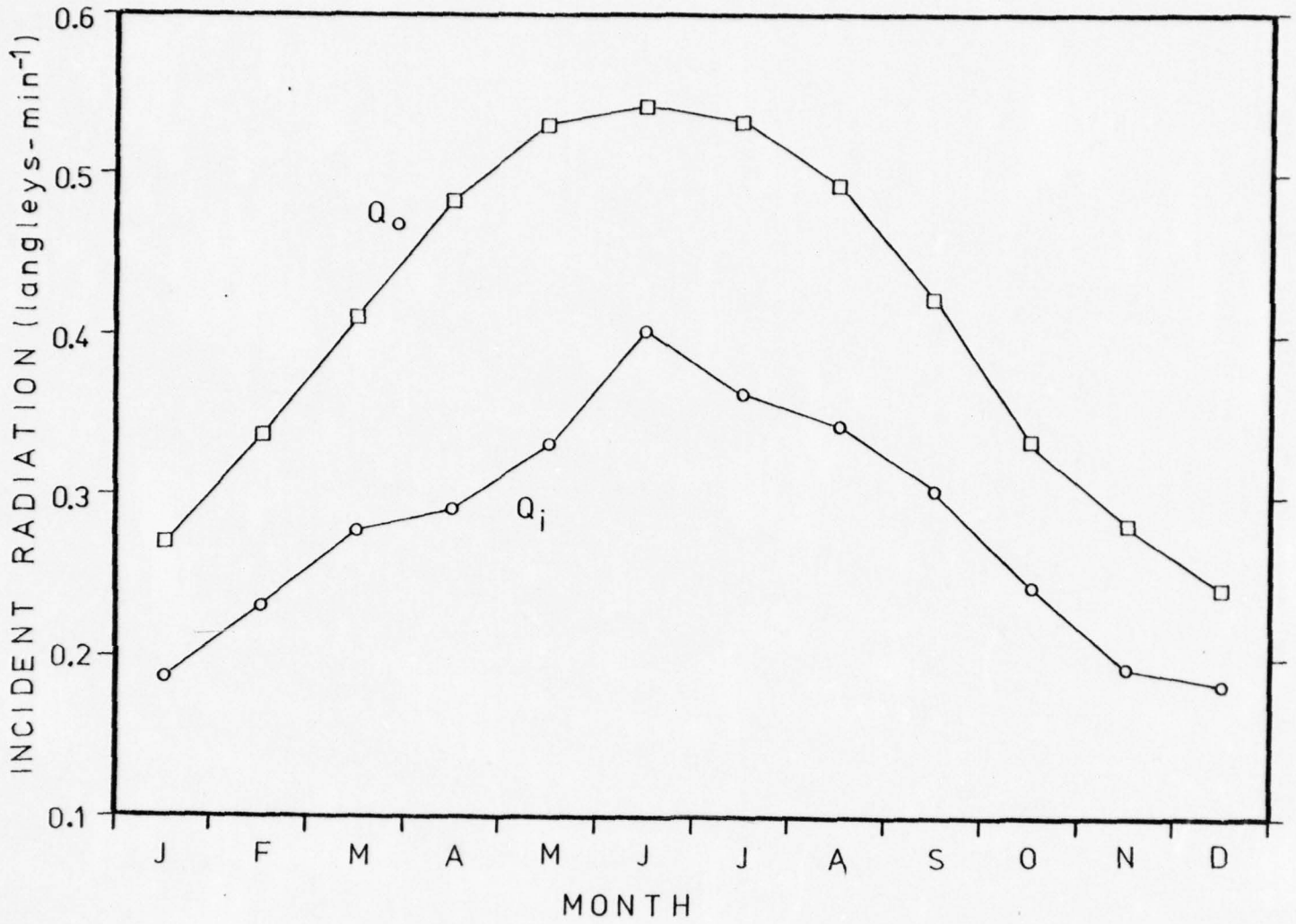

Figure 6. Seasonal variation of incident solar radiation, clear sky conditions (Q_o) and reduced by fog and clouds (Q_i).

The incident solar radiation is an essential part of the ecosystem simulation model in that it is used in the equations governing the production of organic carbon by the photosynthetic activity of phytoplankton. These equations are discussed in detail by Pearson (1975).

C. ALGAL SINKING TERM

The phytoplankton sinking term which was added to the Pearson (1975) model is written in the form used by Riley (1965) in the units of the quantity of phytoplankton transferred per day (g C/m^2-day). The amount of phytoplankton that sinks out of the mixed layer in a day is given by:

$$SINK = (V/Z)X2 \qquad (26)$$

where: SINK = flux of phytoplankton out of mixed layer (gC/m^2-day)

V = sinking rate (m/day)

Z = mixed layer depth (m)

X2 = phytoplankton biomass in mixed layer (gC/m^2)

V/Z = fraction of phytoplankton which sinks out of mixed layer per day

Vertical circulation with the water column becomes significant as the upwelling current speed and sinking rates of phytoplankton approach the same order of magnitude. Since the phytoplankton are non-mobile and are generally of the same density as the water or have developed shapes which increase their sinking resistance, they will be carried along with vertical currents in the water column. The vertical circulation during upwelling opposes sinking but may

accelerate downward transfer during brief periods of surface convergence and associated downwelling.

The complete phytoplankton sinking term is:

$$SINK = ((V - W)/Z)X2 \qquad (27)$$

where: W = upwelling speed (m/day)

An average value of one meter per day was used for the sinking rate (V) in the computer simulation model. This value was determined from estimates presented by Lehman et al. (1975) and Bannister (1974). The SINK term acts to decrease the phytoplankton concentration in the modeled region and is subtracted in the phytoplankton equation (2) as shown:

$$\frac{d\ X2}{dt} = PROD - RESP2 - GRAZ - SINK \qquad (28)$$

D. PHYTOPLANKTON ADVECTION TERM

An equation describing the horizontal advection of phytoplankton is included in the revised model. This term is in the units of flux and is written as:

$$ADVEC2 = W\ (X2)K \qquad (29)$$

where: ADVEC2 = the change of concentration of phytoplankton over time (in the mixed layer) due to advection (g C/m^2-day)

W = upwelling speed (m/day)

X2 = phytoplankton concentration in the mixed layer (g C/m^2)

K = advection coefficient (m^{-1})

The simplified advection term used in the model is derived from the equation (21) shown in the background theory section, which is:

$$\text{Advective change} = W\,(X2)\,\left[-\frac{L}{D\Delta X} + \frac{1}{\Delta Z}\right] \qquad (21)$$

The Ekman current offshore which results in an upwelling current (W) is effective over the depth of frictional resistance (D), but the phytoplankton in the model (which are uniformly distributed in the mixed layer) will be advected at the average velocity over the depth of the mixed layer as determined by the fraction of the mixed layer that is coincident with the Ekman layer. It is known that the mixed layer varies seasonally from about 10 to 100 meters in depth and this causes an annual (seasonal) variation in the average horizontal current in the phytoplankton advection term. The average current of the mixed layer can be determined from:

$$\bar{U} = \frac{1}{Z}\int_{o}^{Z} U_Z dZ \qquad \text{where: } U_Z = \text{a function of } e^{-\pi Z/D} \qquad (30)$$

A shallow mixed layer experiences higher average velocities than a deep layer as seen from the integral expression (eq. 30).

A coefficient to describe the seasonal average of the vertically averaged horizontal current in the mixed layer is included in the advection equation as shown:

$$\text{Advective change} = W\,(X2)\,\left[-\frac{L}{D\Delta X}\,K_m + \frac{1}{\Delta Z}\right] \qquad (31)$$

The coefficient, K_m, represents the seasonal average of the fraction of the mixed layer which is coincident with the Ekman layer and is affected by the Ekman current.

The constants in the advection expression (within the brackets of eq. 31) are lumped into the advection coefficient, K, for convenience in equation (29). The range of K varies from about 10^{-1} to 10^{-2} m^{-1} depending on the estimated values of the gradient distance, (ΔX) and (ΔZ) and the velocity coefficient, K_m. A value of 0.1 m^{-1} was used in this model for K.

E. PREDATION LOSS

The predation pressure function hypothesized for Monterey Bay is based on the assumption that the system supports a resident population of herbivorous zooplankton predators throughout the year. The pressure exerted on the herbivore prey by this maintenance level (N) of predators follows the curve in Figure 7 below the prey density threshold, d. The pressure is sufficiently low to allow growth of the zooplankton stock, but high enough to stabilize growth. A second pressure is imposed on the zooplankton (see Figure 7) after their density reaches the critical level, d. The simulation approximates conditions which may be brought about as transient predators move into the area presumably in response to increased food availability. In summary, predation pressure may be represented by a two part function with a pressure-density curve, a, due to resident predator species and curve b due to the transient predator population.

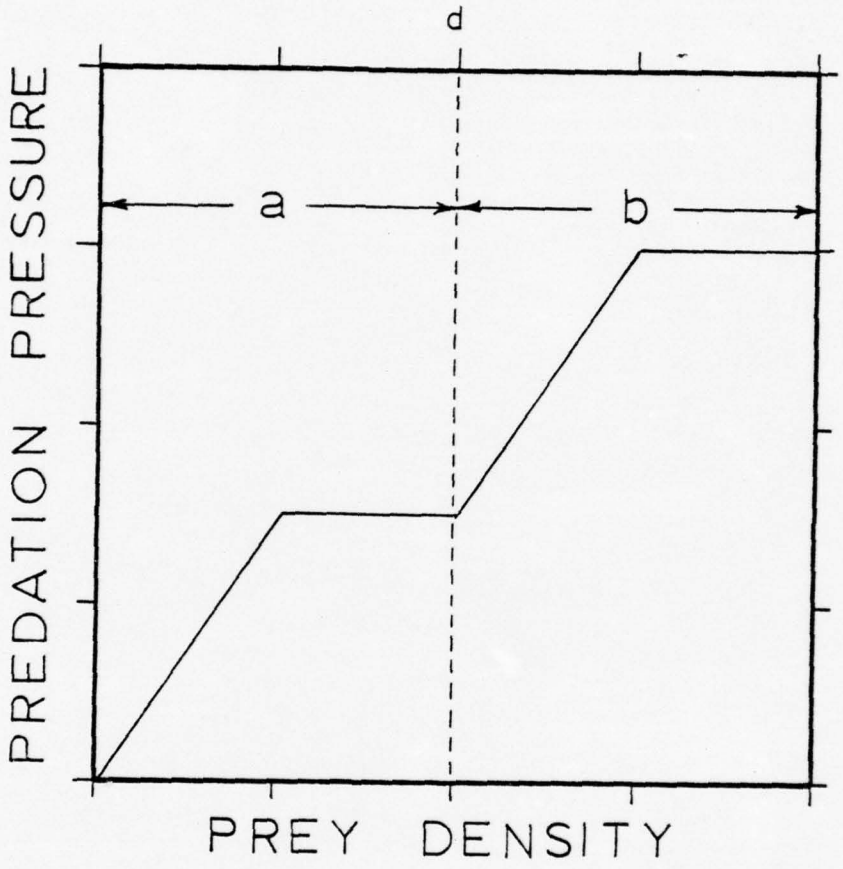

Figure 7. Predation pressure on zooplankton by transient predators.

Predator biomass may be expressed as shown in Figure 8, as a simple step increase or some other function of prey density. Consideration of the step type function is important because it allows the predator population (and consequent pressure) to maximize during those seasons when the zooplankton "standing crop" will support additional numbers of predators; the high predator pressure will deplete the food stock to a lower level than would be reached by the resident predator pressure alone. Measurements of zooplankton biomass for 1974 (Traganza, 1975) suggest a rapid decline in "standing crop" following an early summer maximum. One might suspect that a transient predator population is forced out of the region once the food sources are depleted. This is done in the model by decreasing the predator population when the zooplankton biomass declines to a specified level. The predator levels were related directly to zooplankton "standing crop" by triggering an increase in predator population at a threshold of zooplankton biomass during periods when this prey population was on the upswing. The predators were similarly reduced at a second threshold during the declining phase of zooplankton growth. A set of four conditional statements is used in the simulation to describe the predator-prey relationship. These statements specify the following:

$$\text{IF } \frac{dX3}{dt} > 0 \text{ AND } X3 < 1.0 \text{ THEN: } FISH = 1.0$$

$$\text{IF } \frac{dX3}{dt} > 0 \text{ AND } X3 \geq 1.0 \text{ THEN: } FISH = 5.0$$

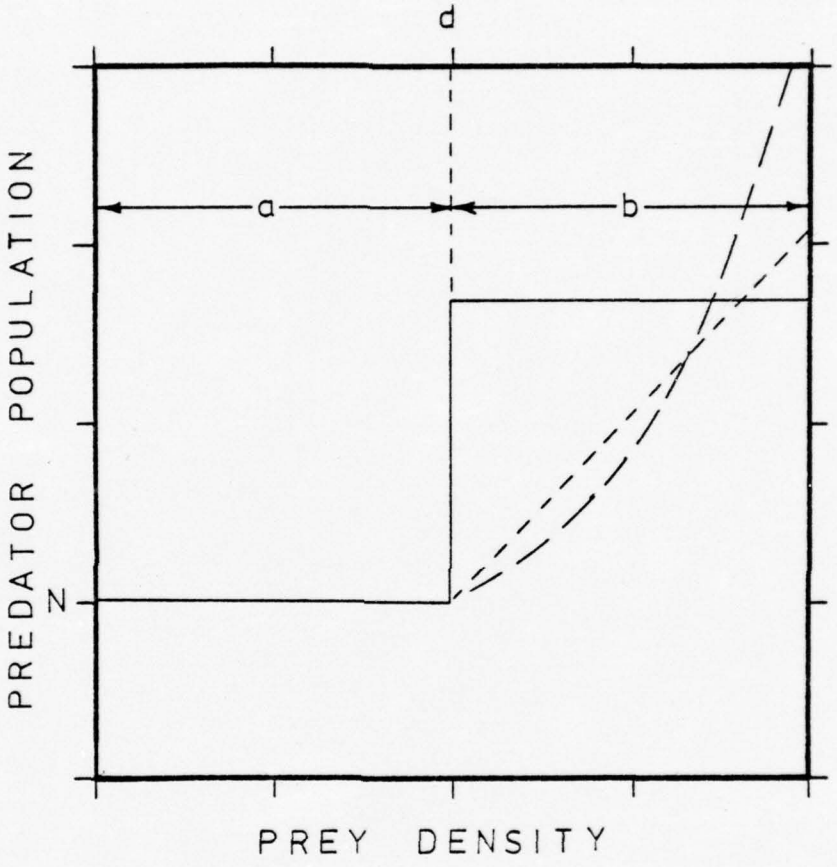

Figure 8. Predator population.

$$\text{IF } \frac{dX3}{dt} \leq 0 \quad \text{AND} \quad X3 \geq 0.2 \quad \text{THEN:} \quad FISH = 5.0$$

$$\text{IF } \frac{dX3}{dt} \leq 0 \quad \text{AND} \quad X3 < 0.2 \quad \text{THEN:} \quad FISH = 1.0$$

The modified predation pressure term in the zooplankton equation of the model is:

$$LOSS = (L)(FISH)(X3) \tag{32}$$

where:

LOSS = the amount of herbivorous zooplankton biomass lost per day as a result of predation ($g\ C/m^2$ day)

L = loss rate or percent loss per FISH per day (day^{-1})

FISH = number of predators (non-dimensional)

X3 = zooplankton "standing crop" ($g\ C/m^2$)

IV. RESULTS

A. UPWELLING CALCULATIONS

The mesoscale wind data used to calculate upwelling for this simulation is shown by Figure 9. The plot depicts the frequency of occurrence ($f = N/\Sigma N$) for 45-degree segments of the compass. The prominent wind direction is as usual from the northwest during the April to September upwelling period and shifts to the south in the first and last quarters, but this year there was a significantly high frequency of northwesterly winds during the last months of the year. The computer generated upwelling index (Figure 10) shows a primary upwelling maximum in May, a second peak in about mid September and another in mid November. The possibility of a secondary upwelling peak is suggested by temperature observations by Traganza et al. (1976). Figure 11 shows a rise in the isotherms peaking 30 to 45 days after the indicated wind initiated upwelling maximums in May and September. Although the water column does not respond instantaneously to surface wind stress, the delay noted here is excessive (Barham, 1957). The delay may be attributable to the assumption that the winds measured at Monterey Airport are actually representative of the winds over the bay, when in fact they may not be. The delay may also be caused by the lack of sufficient data to accurately depict the seasonal trends of temperature in the water column.

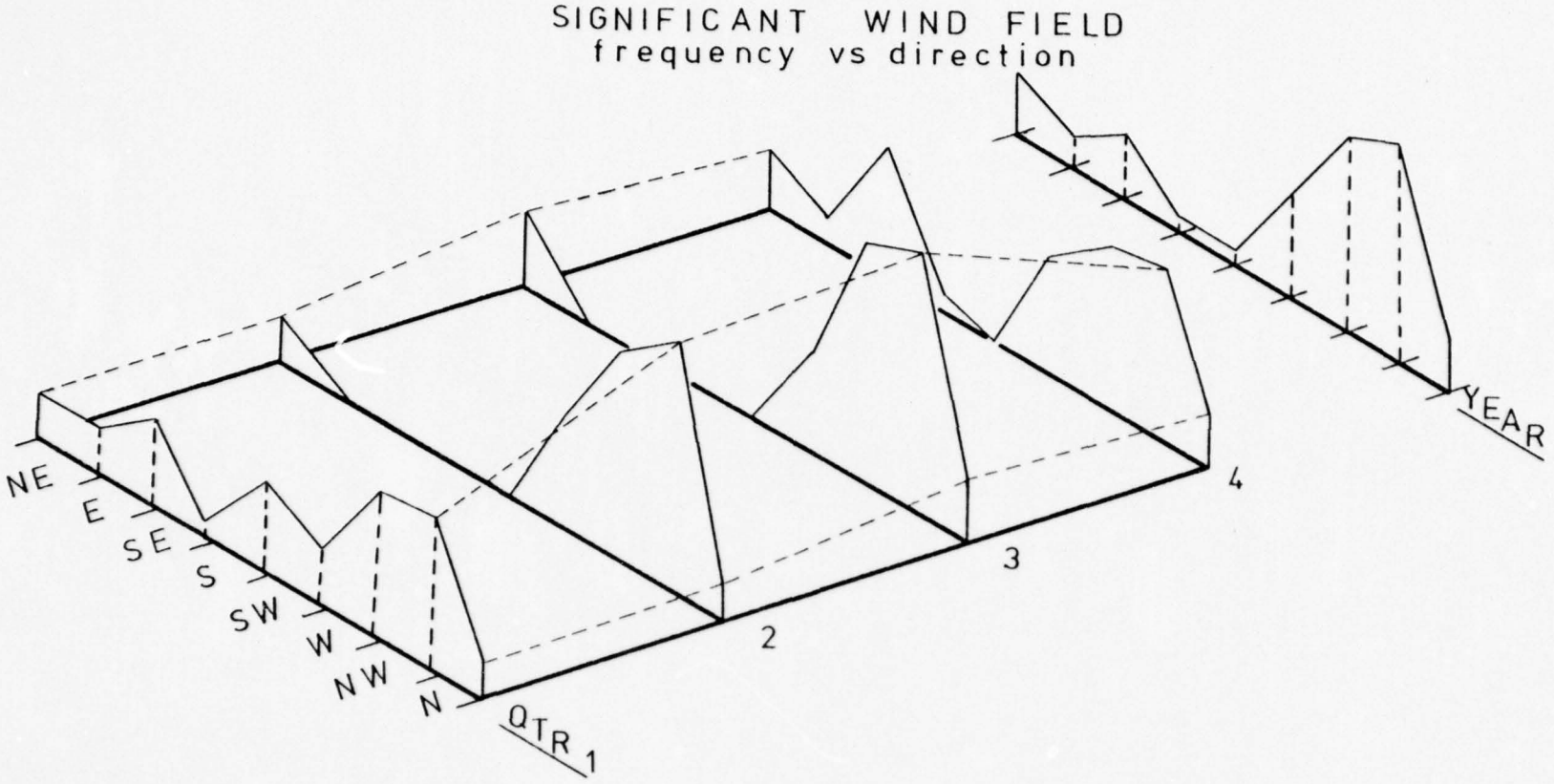

Figure 9. Frequency distribution of wind field direction at Monterey Peninsula Airport, 1974. Wind direction was corrected for topographic effects.

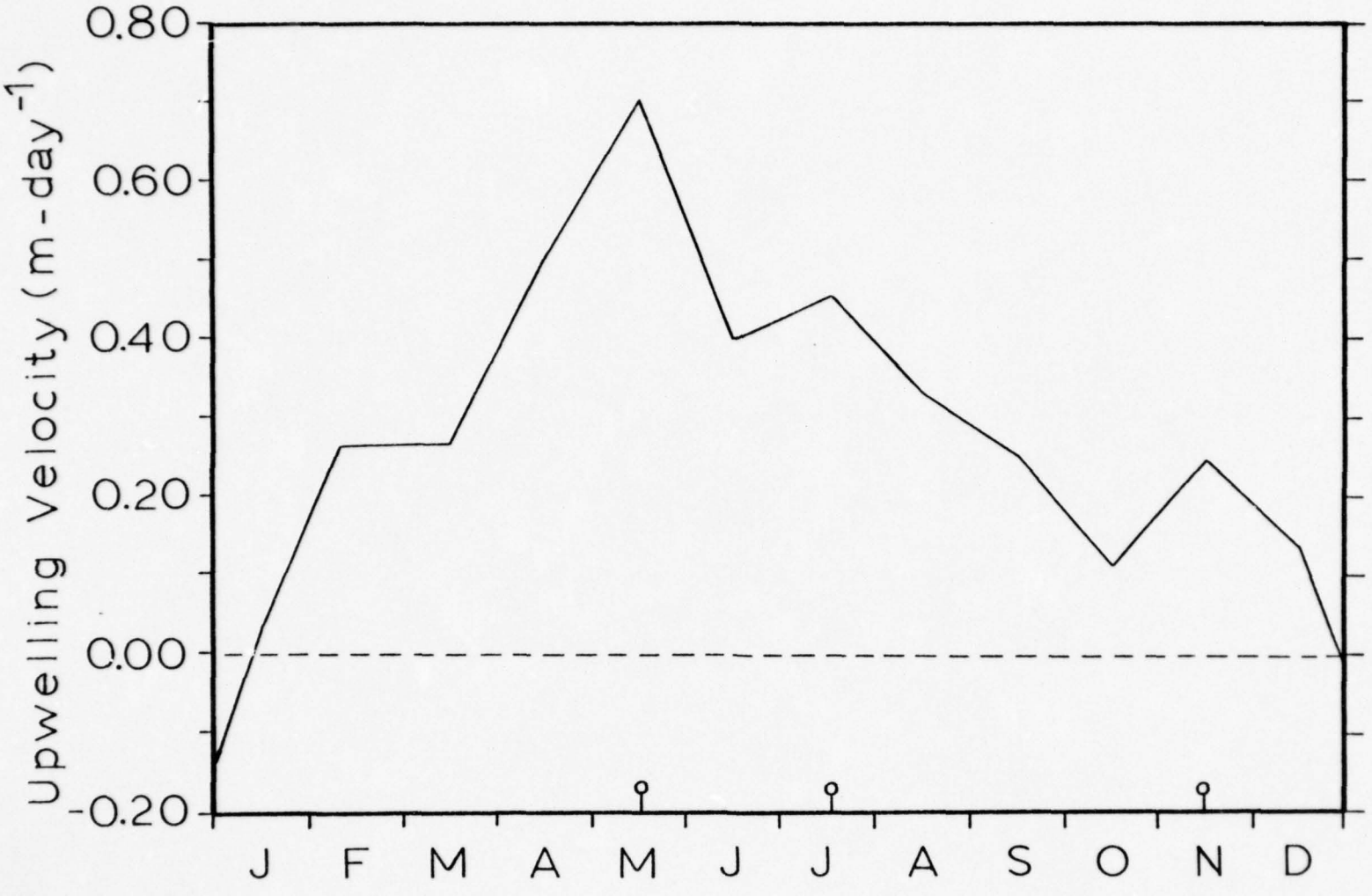

Figure 10. Upwelling index for Monterey from corrected airport wind observations, 1974.

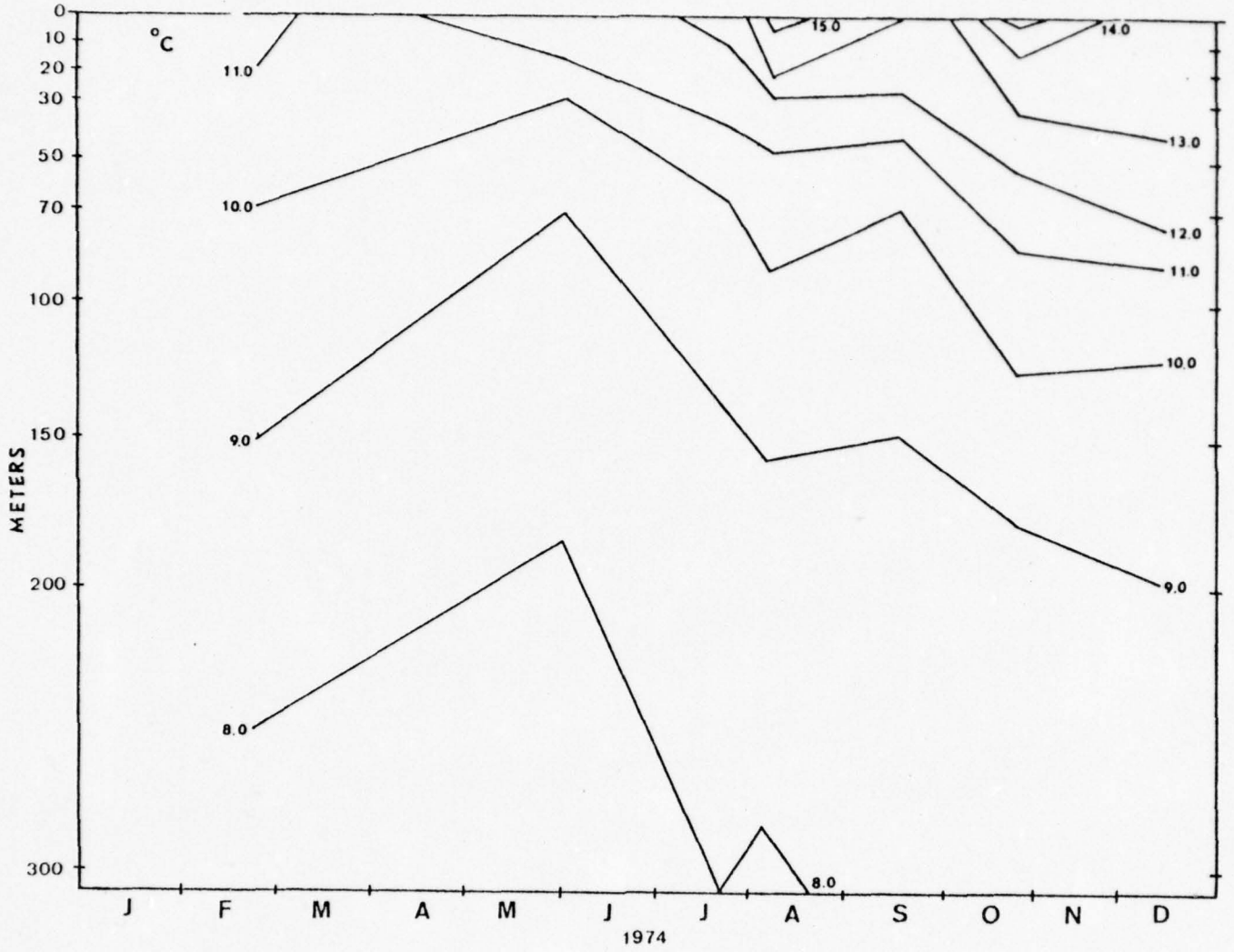

Figure 11. Seasonal temperature variation off Monterey Bay. Values are the mean of four to nine stations (Traganza et al., 1976).

Traganza et al. (1976) observed a sharp rise in phosphate (Figure 12) with the major upwelling in May and a slight increase in phosphate and salinity (Figure 13) in September. No salinity data were available for the first half of the year. There was no clear-cut correlation of either phosphate or salinity to the upwelling index during November. Nutrient data from four to nine stations taken during seven cruises in 1974 were averaged (see Figure 12) and show a rapid rise in October which is probably not related to upwelling. From the five year study of Monterey Bay by Bolin (1964) it is known that the nutrient concentration is characteristically low over the depth of the euphotic zone (0-200 meters) for two or three months at the end of the year. The restoring of the nutrient level in all but the upper 20 to 30 meters to half of its May upwelling value while the surface temperature reached a peak, may have signalled the beginning of the Davidson current period (see Bolin and Abbott, 1962). The Davidson current brings a southerly winter oceanic water mass into the Monterey region. This "Davidson water" is characterized by lower surface temperatures and surface salinities (due to high amounts of rain). The deeper water of the euphotic zone has higher salinities and nutrient concentrations than exist at Monterey. The mechanism which establishes these characteristics may be winter storm mixing occurring south of Monterey or upwelling and mixing from below brought about by divergent (cyclonic) eddies formed in the current stream as it moves northward along the coast (Traganza et al., 1976).

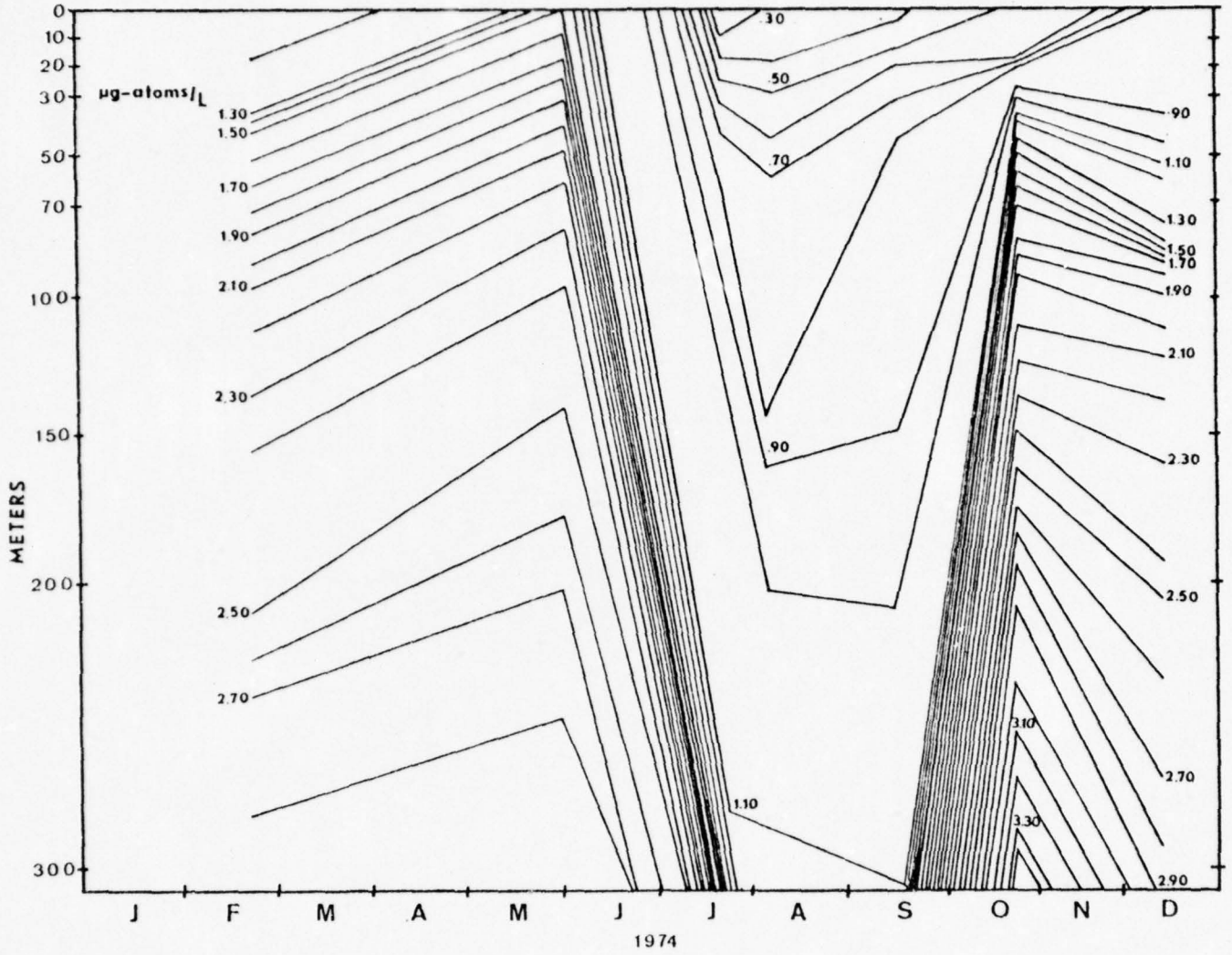

Figure 12. Seasonal phosphate variation off Monterey Bay. Values are the mean of four to nine stations (Traganza et al., 1976).

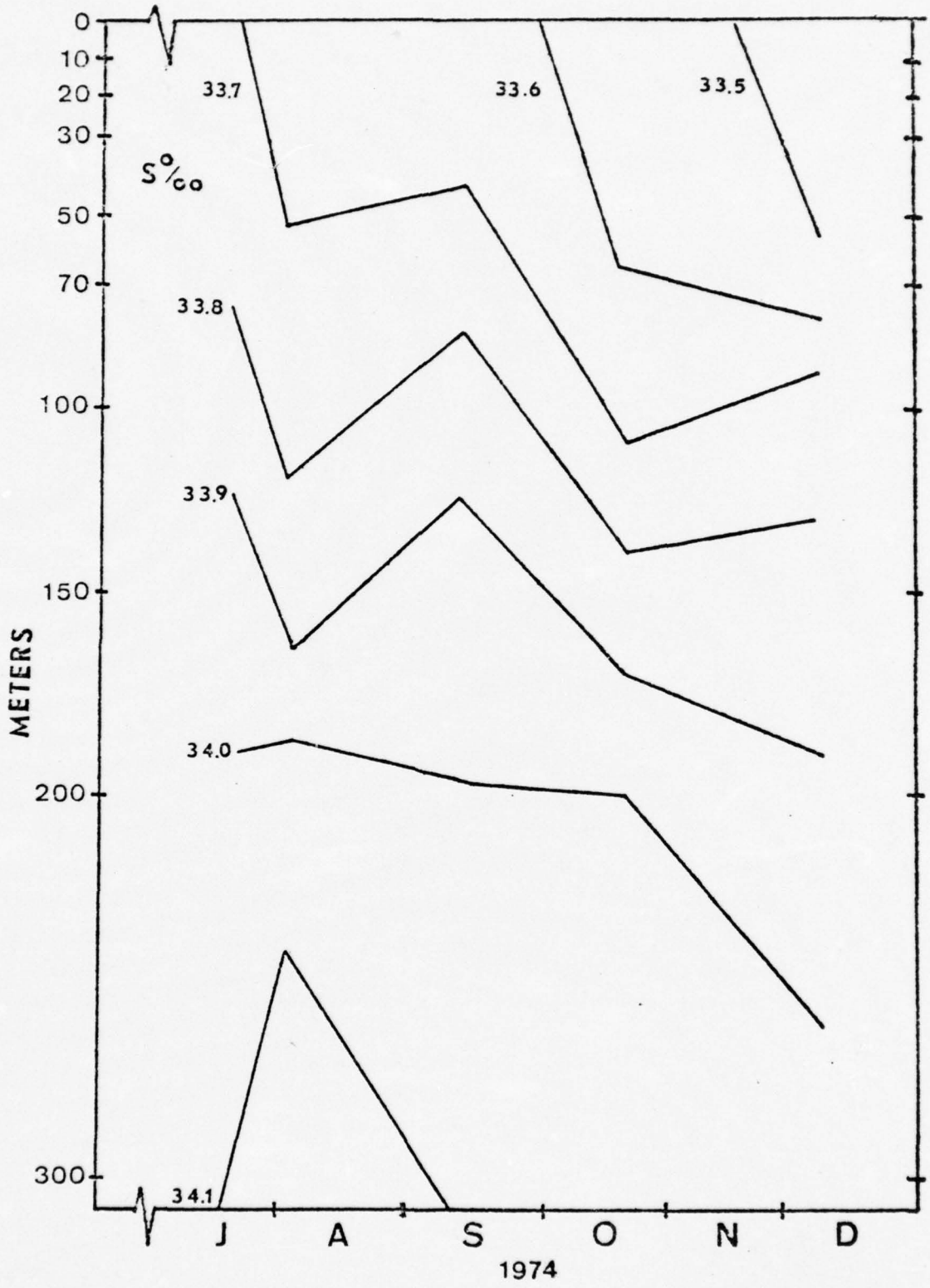

Figure 13. Seasonal salinity variation off Monterey Bay. Values are the mean of four to nine stations (Traganza et al., 1976).

Traganza's (1976) data were obtained at stations in an X pattern referenced to a drogue (Figure 14) and at intervals of about two miles, two and one-half hours apart. The data from four to nine stations were averaged to obtain the values shown in Figures 11, 12 and 13.

Barham (1957) argues that the vertical circulation of Monterey Bay during the upwelling period is characterized by a region of surface divergence coincident with the head of the Monterey submarine canyon. The effect is due to "channeling" of upwelled replacement water along the canyon axis with a plume appearing at the surface near shore (see Figure 15). Evidence in support of this circulation concept is given by a distinct gradient of phytoplankton concentration in the surface waters outlying the canyon head (Barham, 1957). Barham believes that the gradient is due to the rapid horizontal advection of phytoplankton innoculum representing a potential bloom away from the canyon head before the population shows any significant growth. During periods of reduced upwelling as indicated by the trends of the isotherms, phytoplankton counts over the canyon rose to higher values, indicating that surface divergence or horizontal advection had diminished. This possibility should not alter the timing of the model which is related to the general upwelling, but it does suggest serious spatial sampling problems.

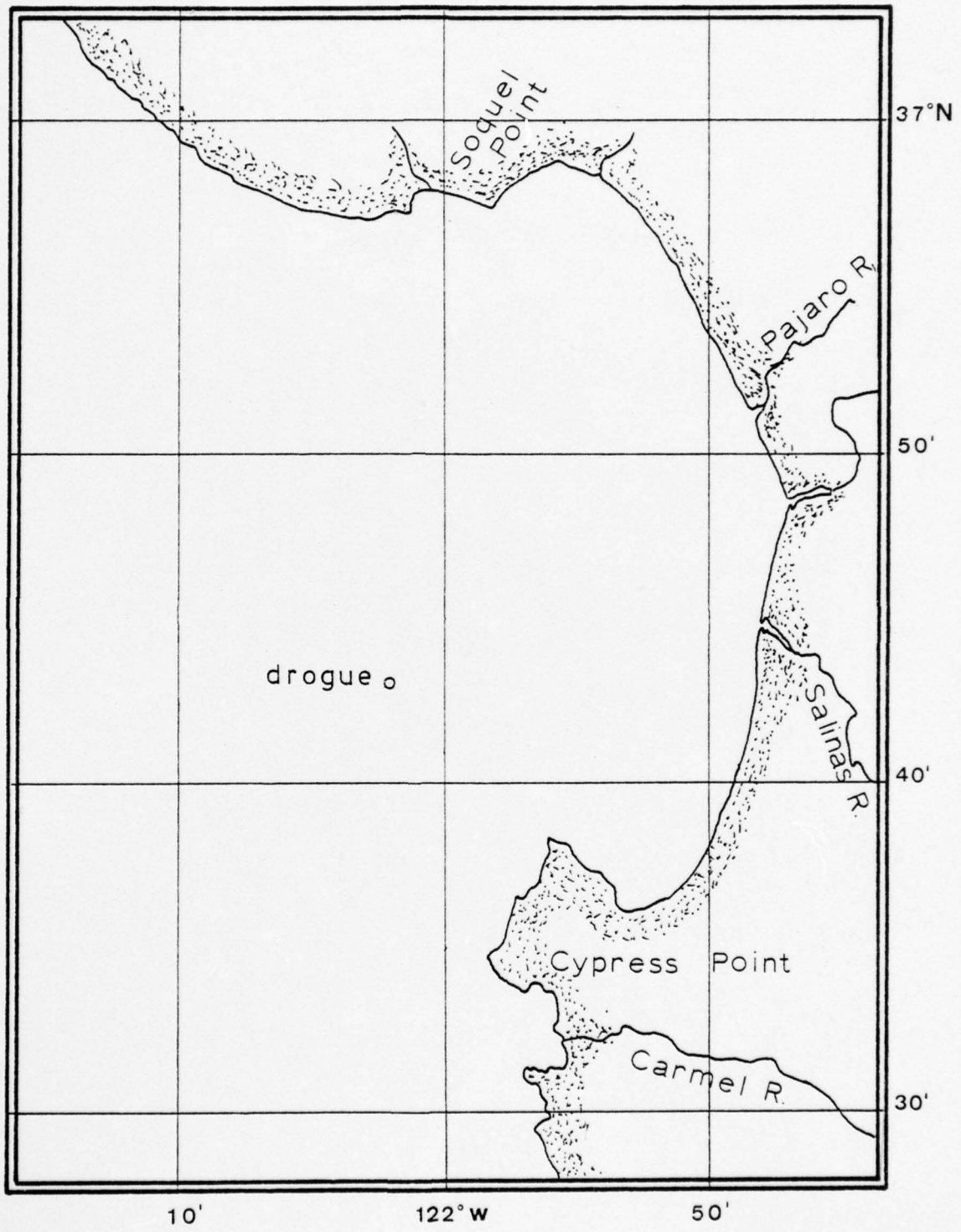

Figure 14. Chart of the Monterey area showing station location.

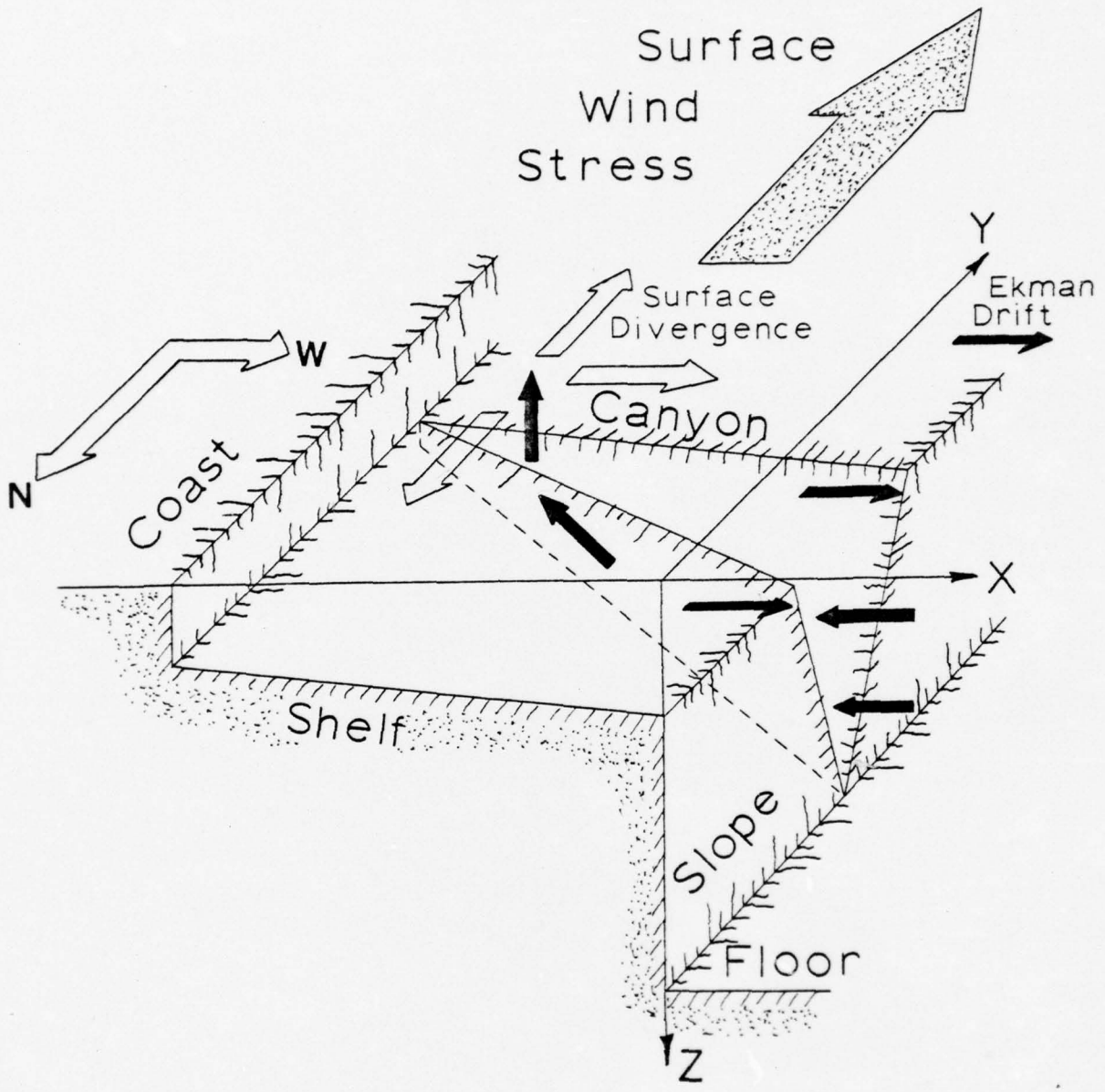

Figure 15. Possible "fountainhead" effect over canyon head.

B. SENSITIVITY ANALYSIS

The model was tested under various conditions of phytoplankton sinking rates, predation pressure on herbivorous zooplankton, and advection of phytoplankton to determine the effect on the simulation of the seasonal cycle phosphate, phytoplankton and herbivorous zooplankton.

Losses of phytoplankton by sinking and therefore food limitation on zooplankton was examined by setting the predation terms on zooplankton to zero and varying the rate of sinking of algal cells, i.e. the availability of food. Sinking rates of zero, three, and six meters per day were used (Parsons and Takahashi, 1973 and Riley, 1965). The effects are shown in Figures 16, 17, and 18. Under conditions of zero sinking, a rapid rise in zooplankton "standing crop" in late summer reduces the phytoplankton biomass quickly to a minimum on day 215. The large decrease in phytoplankton allows the nutrient concentration to remain at a relatively high level (Figure 16) since the uptake of nutrients by phytoplankton is decreased while ongoing zooplankton excretion and mixing by upwelling add to the nutrient concentration. The rate of growth of the herbivorous zooplankton population or "standing crop" is shown to decrease with progressively higher phytoplankton sinking rates (Figure 18) as does the magnitude of the maximum zooplankton biomass reached during the year. The maximum also occurs later with increased sinking rate.

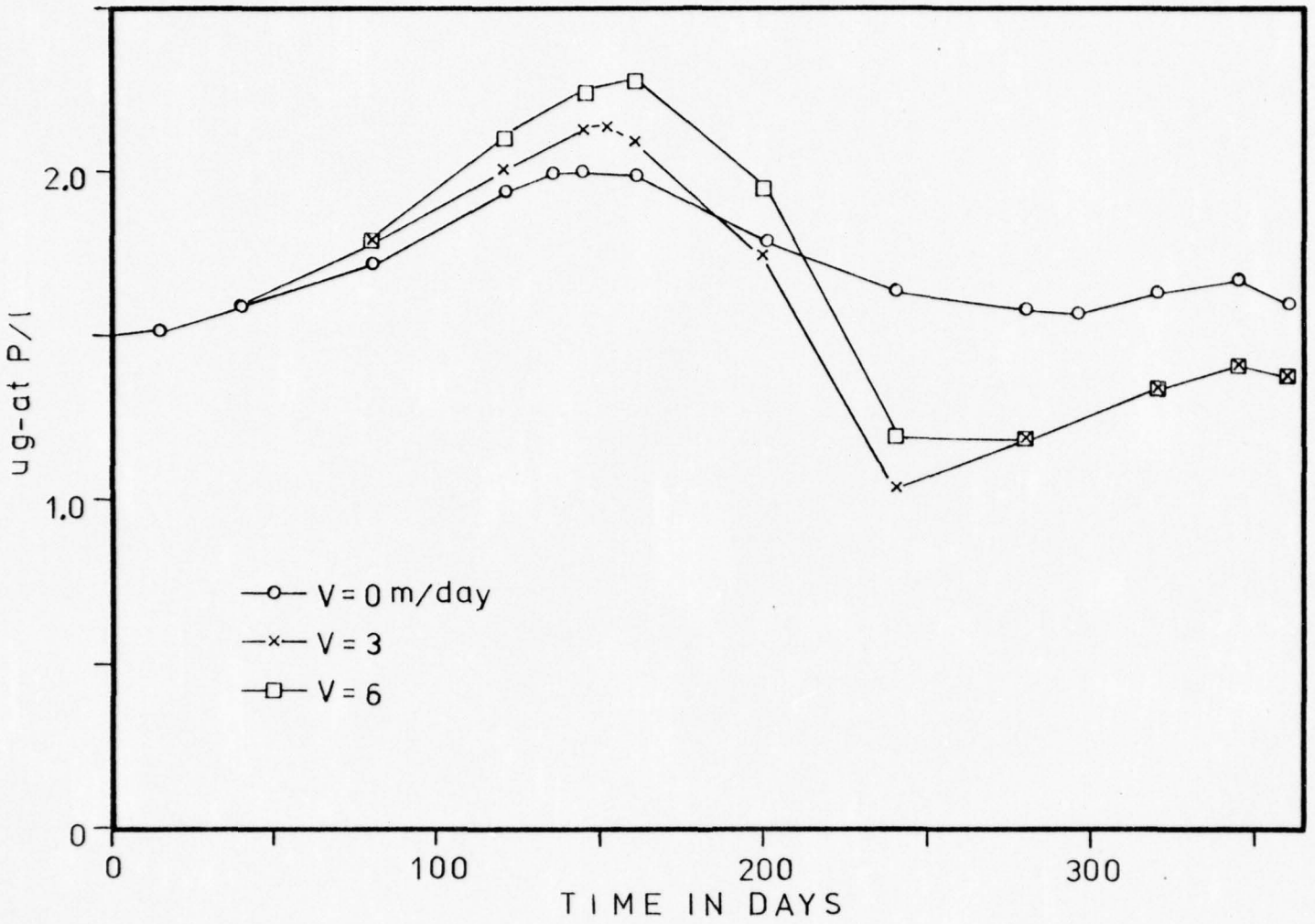

Figure 16. Simulated seasonal phosphate concentration with various phytoplankton sinking rates; no predation.

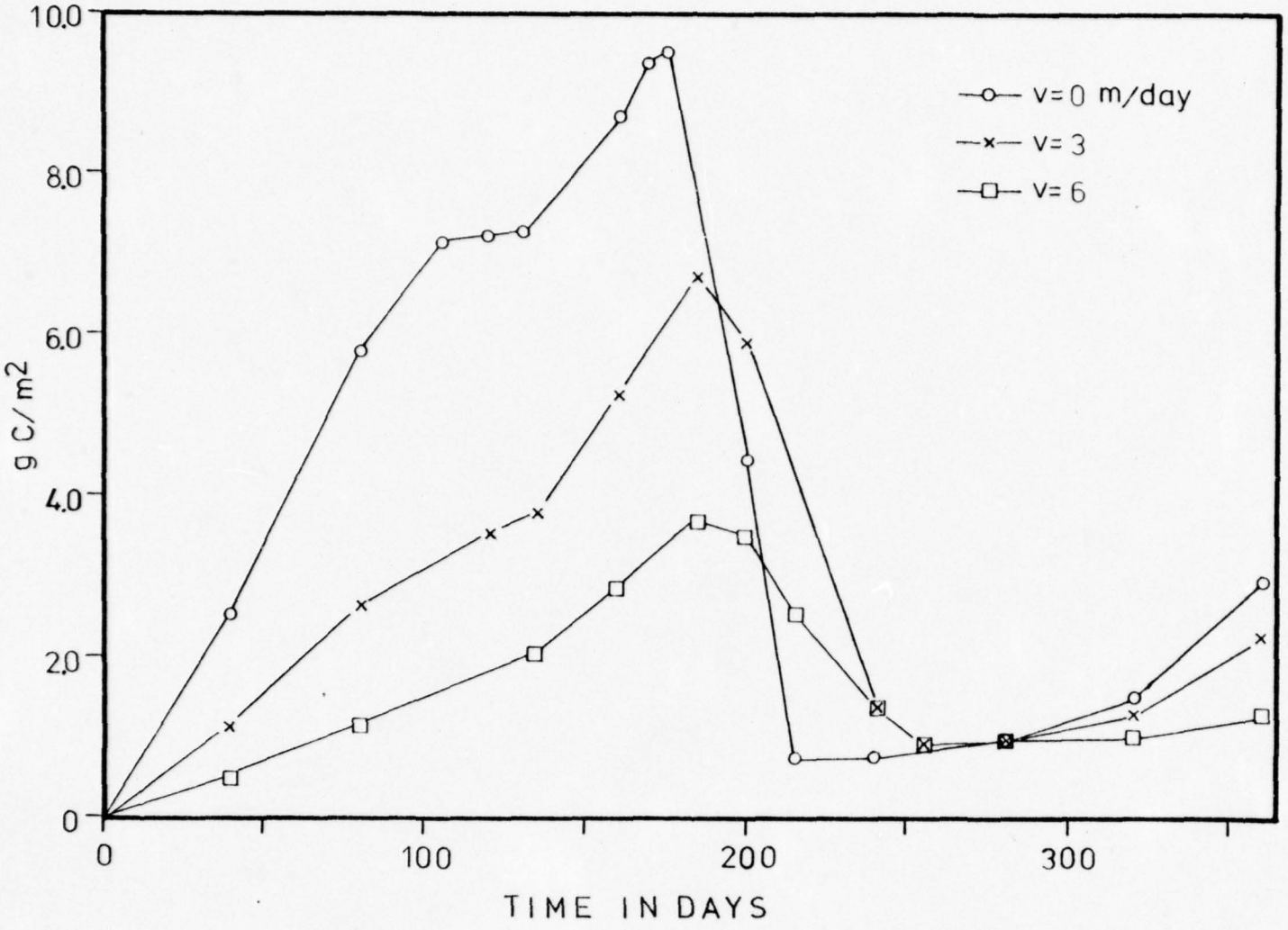

Figure 17. Simulated seasonal phytoplankton concentration with various phytoplankton sinking rates; no predation.

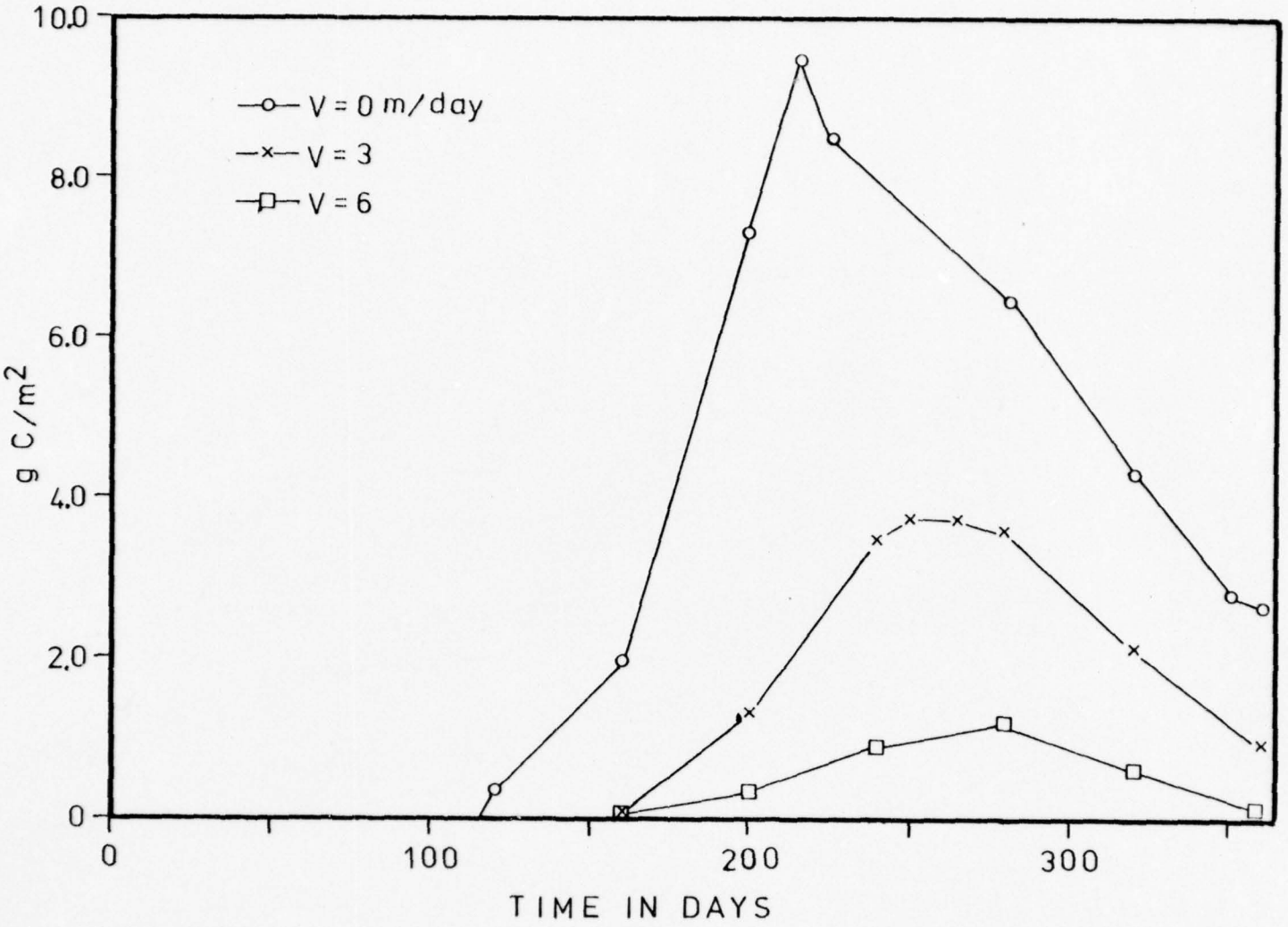

Figure 18. Simulated seasonal zooplankton concentration with various phytoplankton sinking rates; no predation.

The sinking rate was varied in a second test but predator pressure was exerted on the zooplankton by employing the step function predator-prey relationship detailed earlier. Additional predators were introduced in the simulation at a zooplankton biomass level of 1.0 g C/m^2 and were removed when zooplankton biomass fell to 0.2 g C/m^2. Threshold values were determined empirically. The zooplankton biomass maximum is reduced from 1-10 g C/m^2 to 0.1-1.0 g C/m^2 by the addition of predation pressure (Figure 21). The phosphate curves (Figure 19) show a marked response to phytoplankton growth as evidenced by a lower nutrient minimum following the peak of the summer bloom. A considerable change in the zooplankton response, i.e. lower and earlier, is evidently due to reduction of food sources as phytoplankton is allowed to sink out of the mixed layer. The initial effect of increasing the sinking rate from zero to three m/day on zooplankton is a shift in the occurrence of the peak to approximately 70 days later. Further increase of the sinking rate to six m/day results in a twofold decrease in the carbon biomass of zooplankton with an additional 20 day delay of the maximum. It is apparent that the rate of growth of zooplankton is slowed down and the maximum biomass occurs later because of food limitation but that predator pressure is responsible for limiting the magnitude of the zooplankton biomass. The zooplankton peaks also occur earlier when predation is applied and also occur before the phytoplankton peaks (Figure 20). The simulation, therefore requires a positive sinking rate.

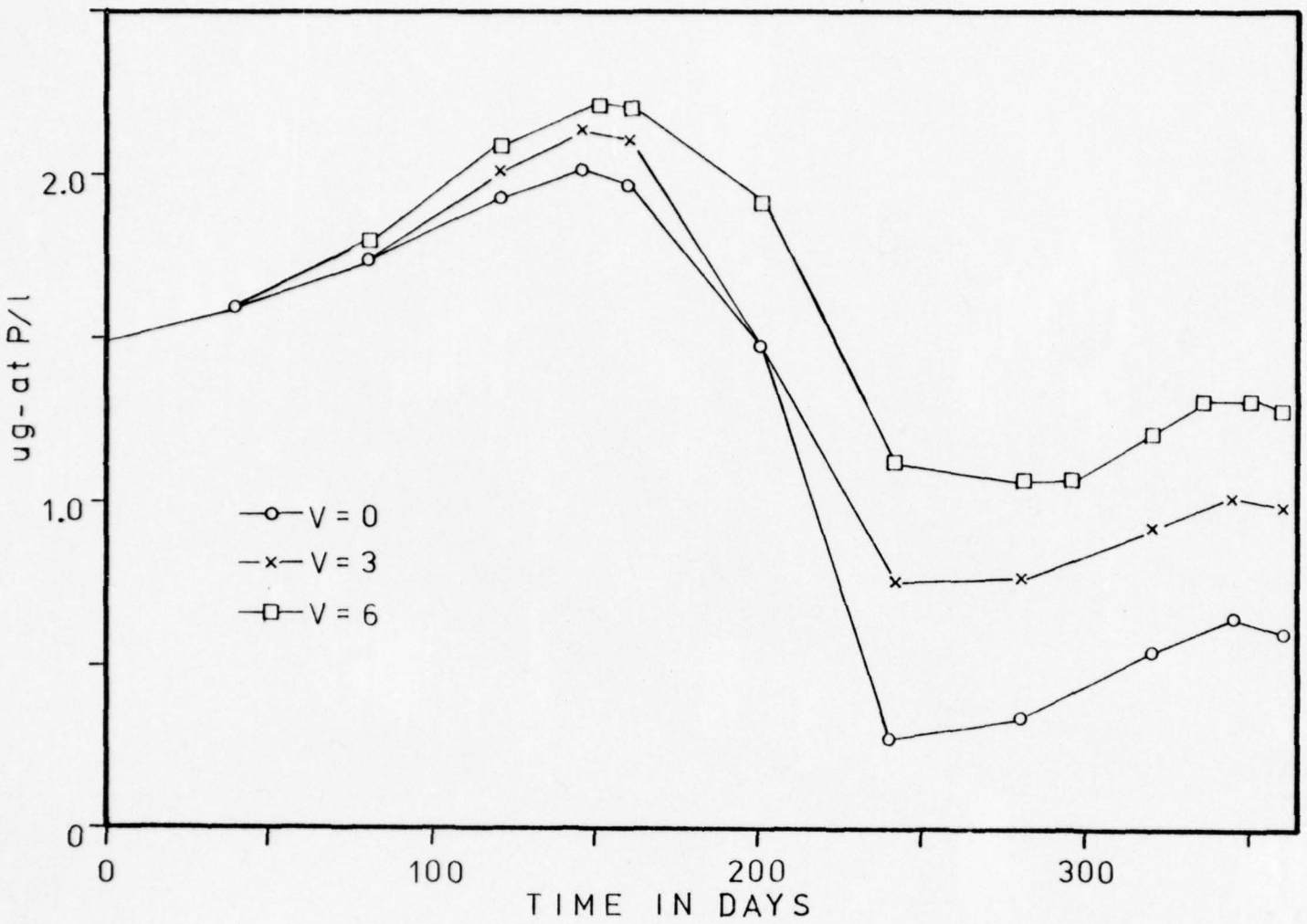

Figure 19. Simulated seasonal phosphate concentration with various phytoplankton sinking rates; with predation.

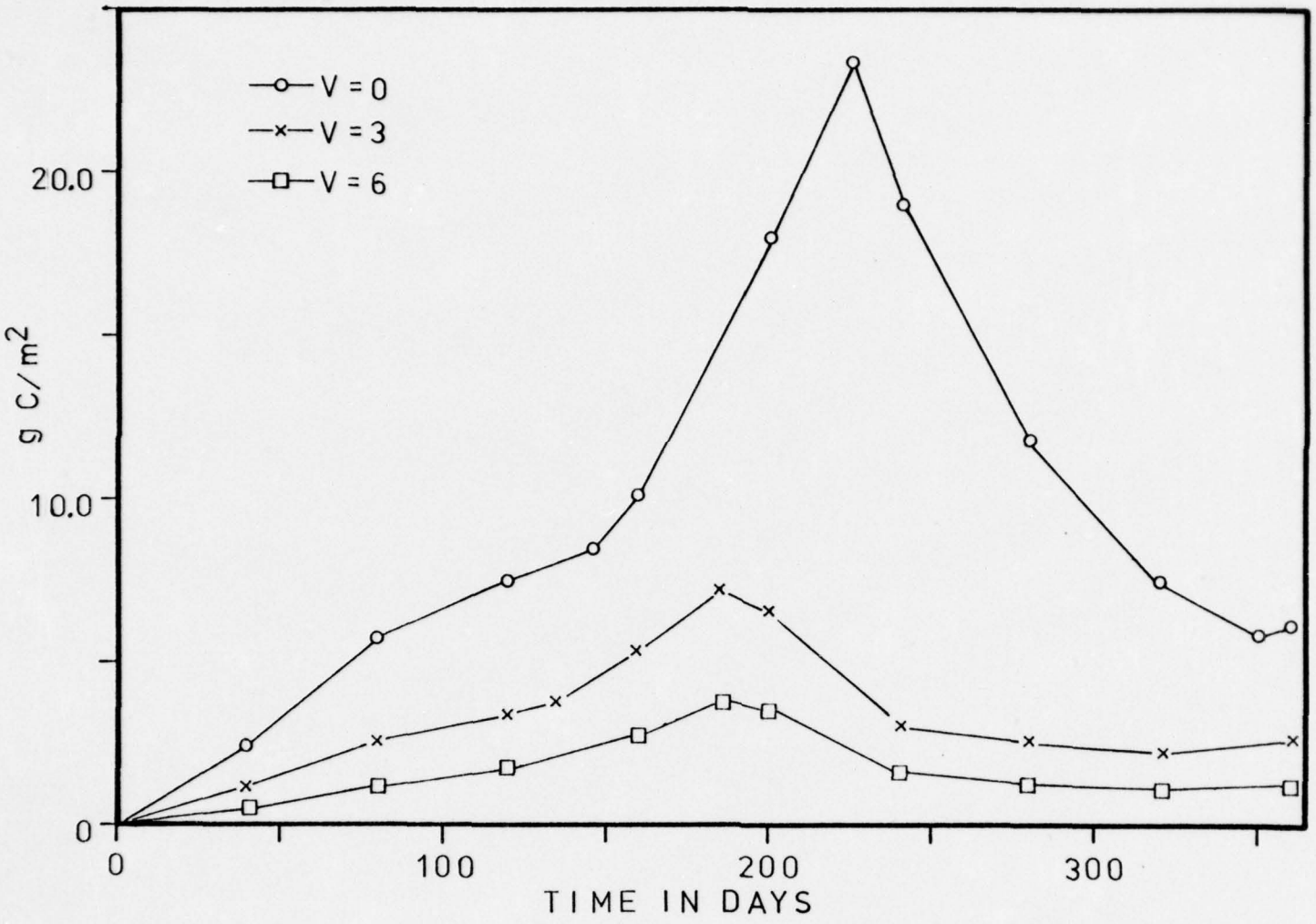

Figure 20. Simulated seasonal phytoplankton concentration with various phytoplankton sinking rates; with predation.

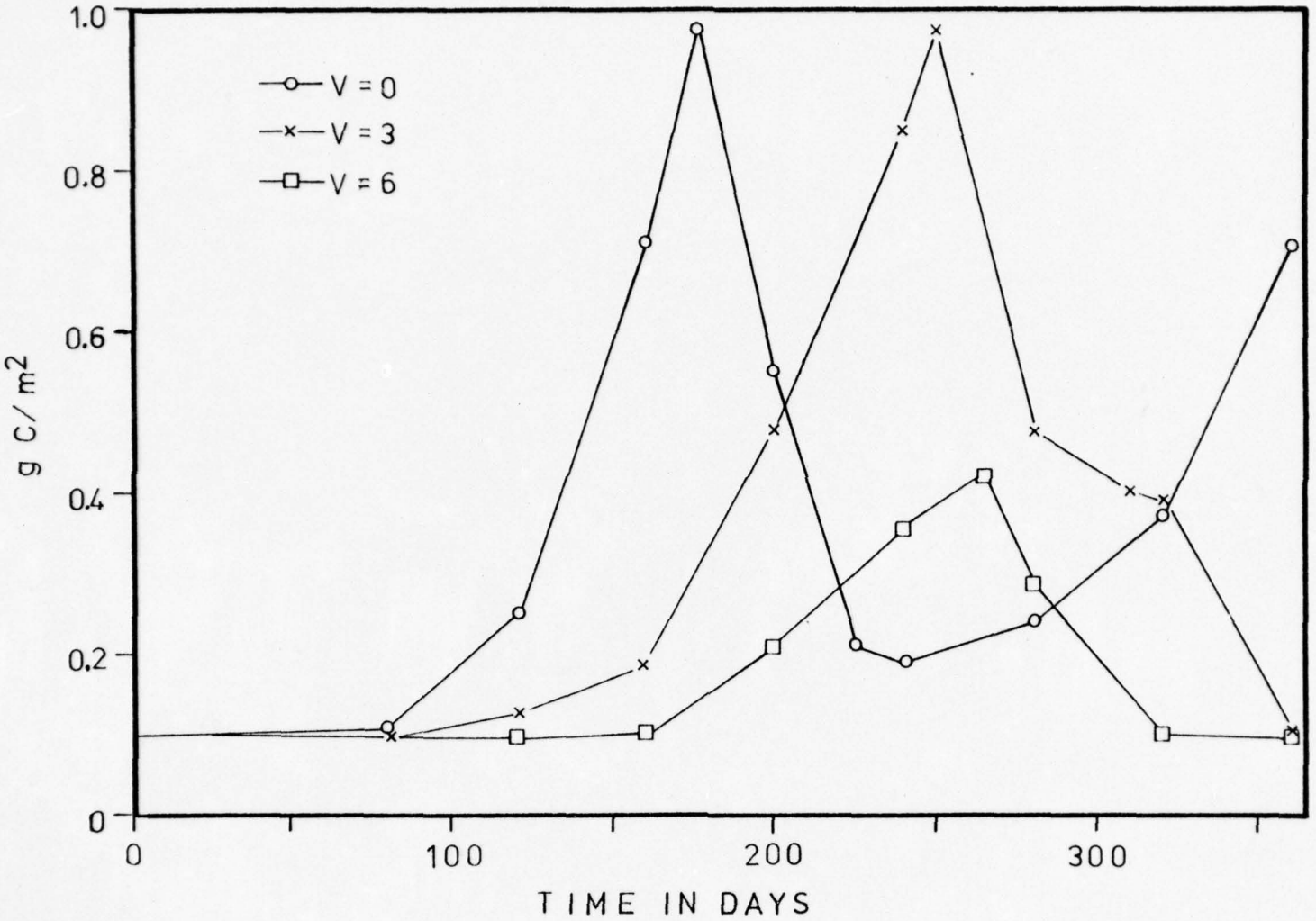

Figure 21. Simulated seasonal zooplankton concentration with various phytoplankton sinking rates; with predation.

The advection rate of phytoplankton was next varied while the sinking rate was held constant at 1.0 m/day (Bannister, 1974) and predator pressure was imposed in the same manner (and with the same thresholds) as in the second test. The results are shown in Figures 22, 23, and 24. A slower rate of growth of zooplankton is produced again when the advection coefficient, K, is increased from 0.0 to 0.3 m^{-1}. Increasing the value of K has the direct effect of increasing the rate of phytoplankton advection. The single maximum of zooplankton simulated under conditions of high advection where K = 0.3 m^{-1} is due apparently to the sensitivity of the model's zooplankton growth equation to the mixed layer temperature and which permits a rapid growth of zooplankton during the mixed layer temperature minimum. The single peak of zooplankton (Figure 24) coincided with a relative temperature minimum about day 260. In Pearson's simulation a ten percent decrease in mixed layer temperature had a marked effect on zooplankton growth. This effect carried over to the partially modified simulation model. The effect of rapid zooplankton growth in a low temperature mixed layer, despite contradicting factors of growth such as low food availability, is due to the sensitivity of the respiration term in the zooplankton growth equation to temperature. This condition is a peculiarity of the model and it is doubtful whether the real ecosystem behaves in the same manner. The zooplankton peak precedes the phytoplankton peak when advection is zero indicating the model needs an advection term.

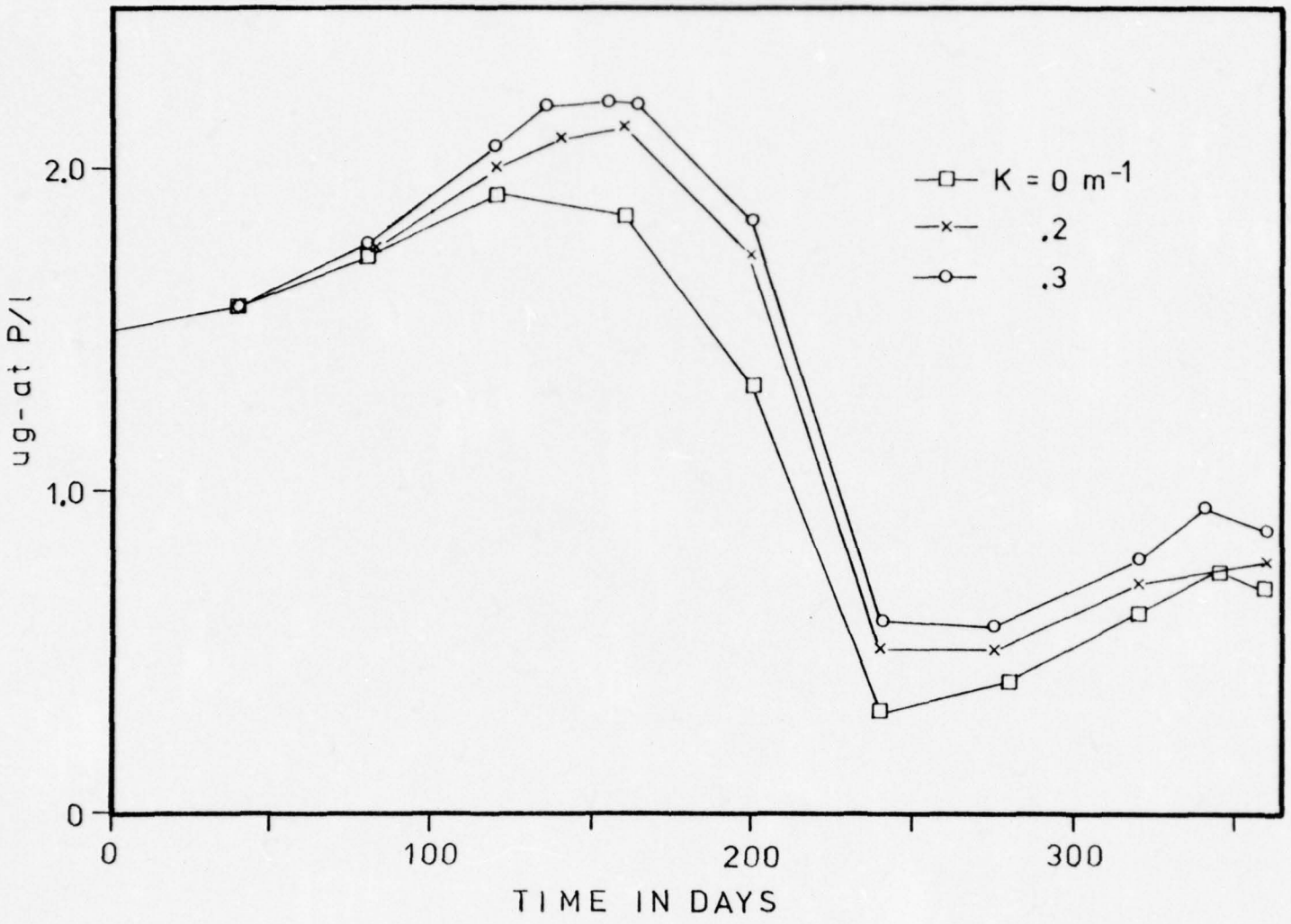

Figure 22. Simulated seasonal phosphate concentration with various phytoplankton advection rates (with predation and algal sinking rate = 1.0 m/day).

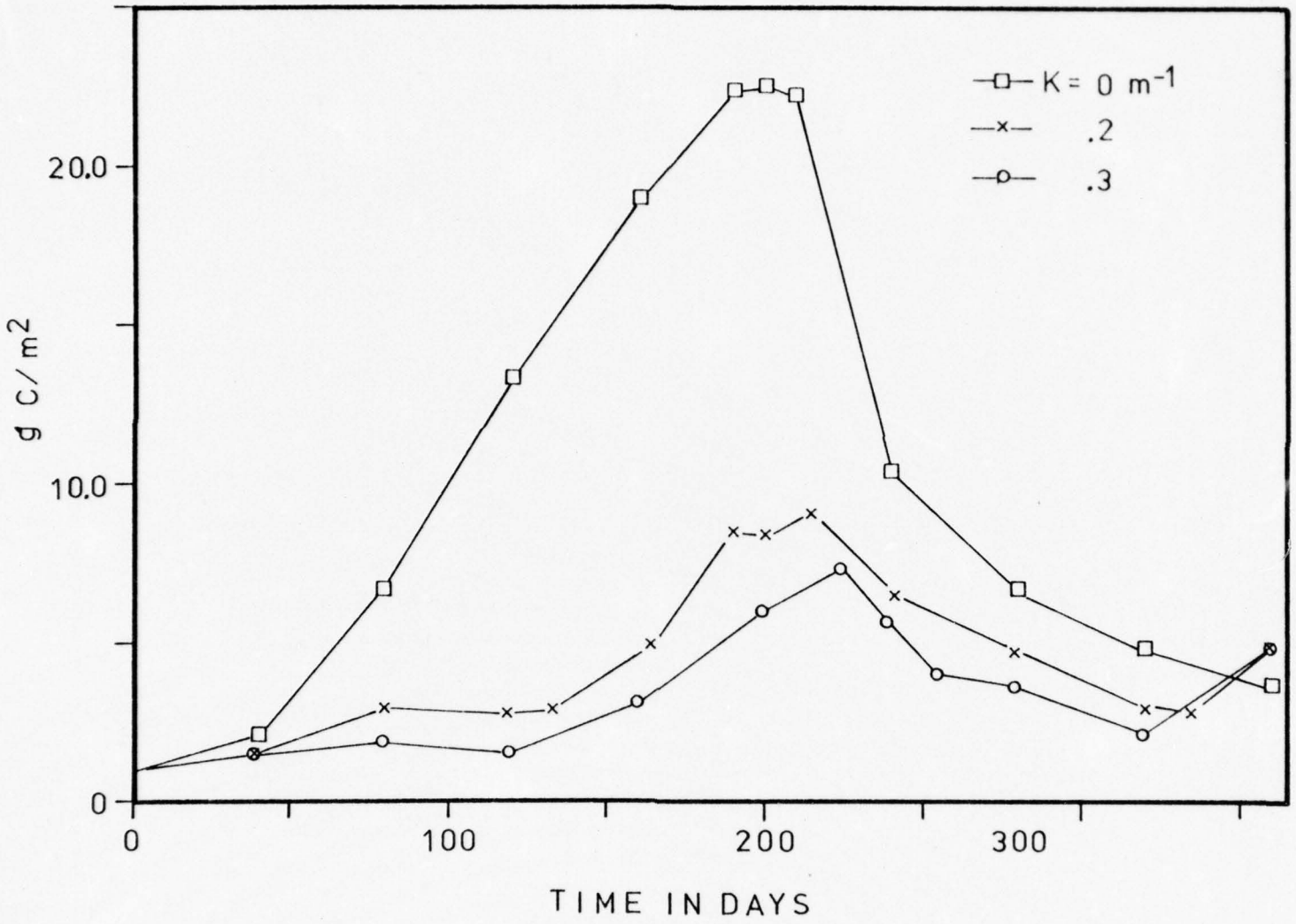

Figure 23. Simulated seasonal phytoplankton concentration with various phytoplankton advection rates (with predation and algal sinking rate = 1.0 m/day).

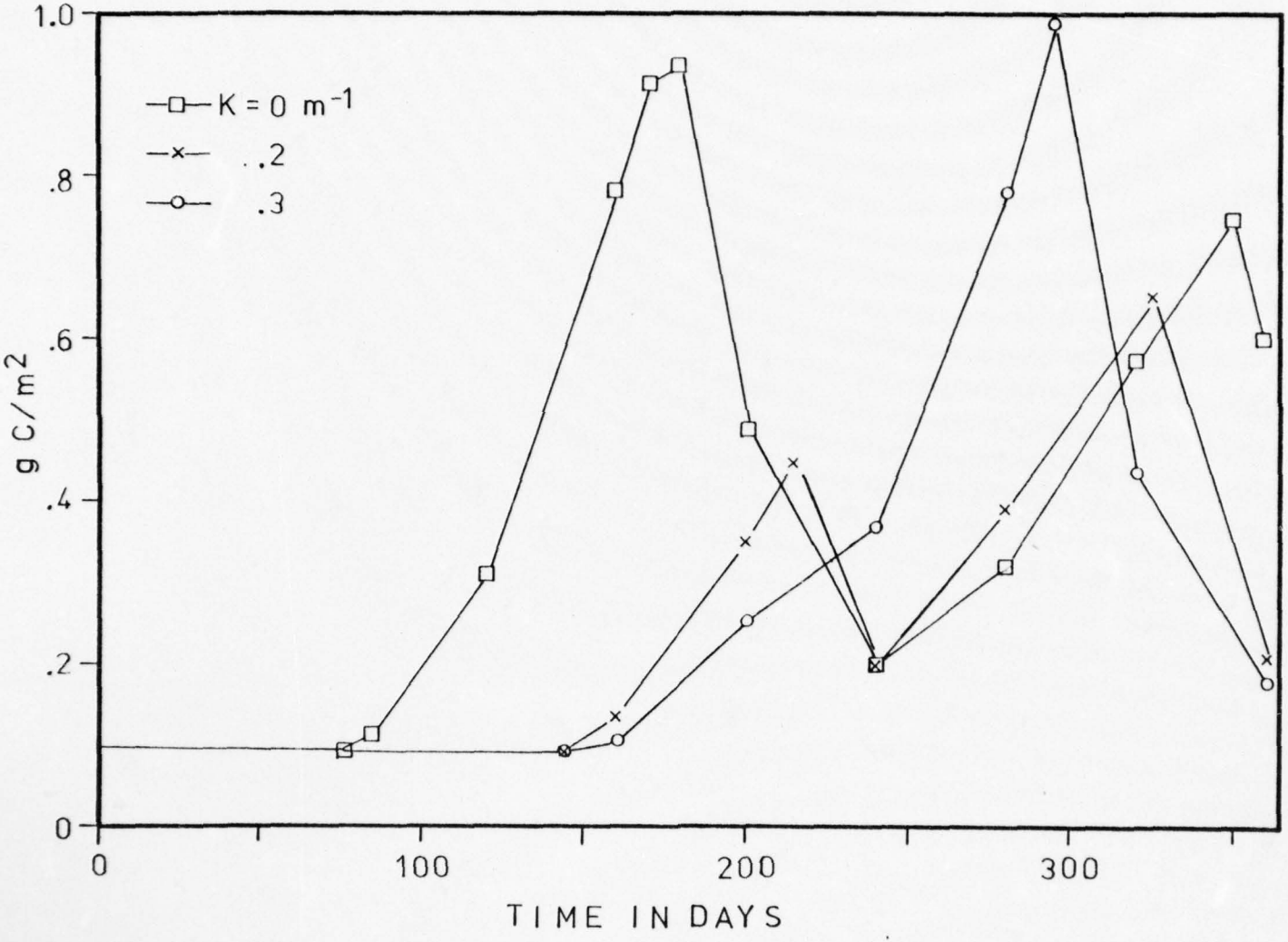

Figure 24. Simulated seasonal zooplankton concentration with various phytoplankton advection rates (with predation and algal sinking rate = 1.0 m/day).

The predation pressure terms in the zooplankton equation were varied (Figures 25, 26, and 27) while keeping the sinking rate at 1.0 m/day and the advection coefficient at K = 0.1 m^{-1}. The conditions of the test were:

1. predation pressure set to zero;
2. predation pressure defined by the linear function of zooplankton biomass: predator pressure = L times zooplankton biomass, where L = 0.01, and the units are g C/m^2-day = $(day^{-1})(g\ C/m^2)$;
3. the linear function in 2, but L = 0.02;
4. the step function discussed under the methods section of this thesis.

In all cases, the resulting zooplankton growth appears food-limited until about day 120 when phytoplankton growth begins to show a rate change. Complete removal of predator pressure allows the zooplankton to increase rapidly until food limitation (be depletion of phytoplankton) again occurs on day 275. When the predator pressure increases linearly (with L = 0.01), a single zooplankton peak of 3.05 g C/m^2 occurs about day 300. This is not consistent with observed conditions (Traganza, 1976). Doubling the predation pressure rate to L = 0.02 day^{-1} severely restricts zooplankton growth but produces a curve with a hint of temporal conformity to the observed zooplankton maximum and minimum biomass levels. When the predator function is triggered at thresholds of zooplankton biomass, the zooplankton exhibit a double peak which is suggested by Traganza's (1976) data.

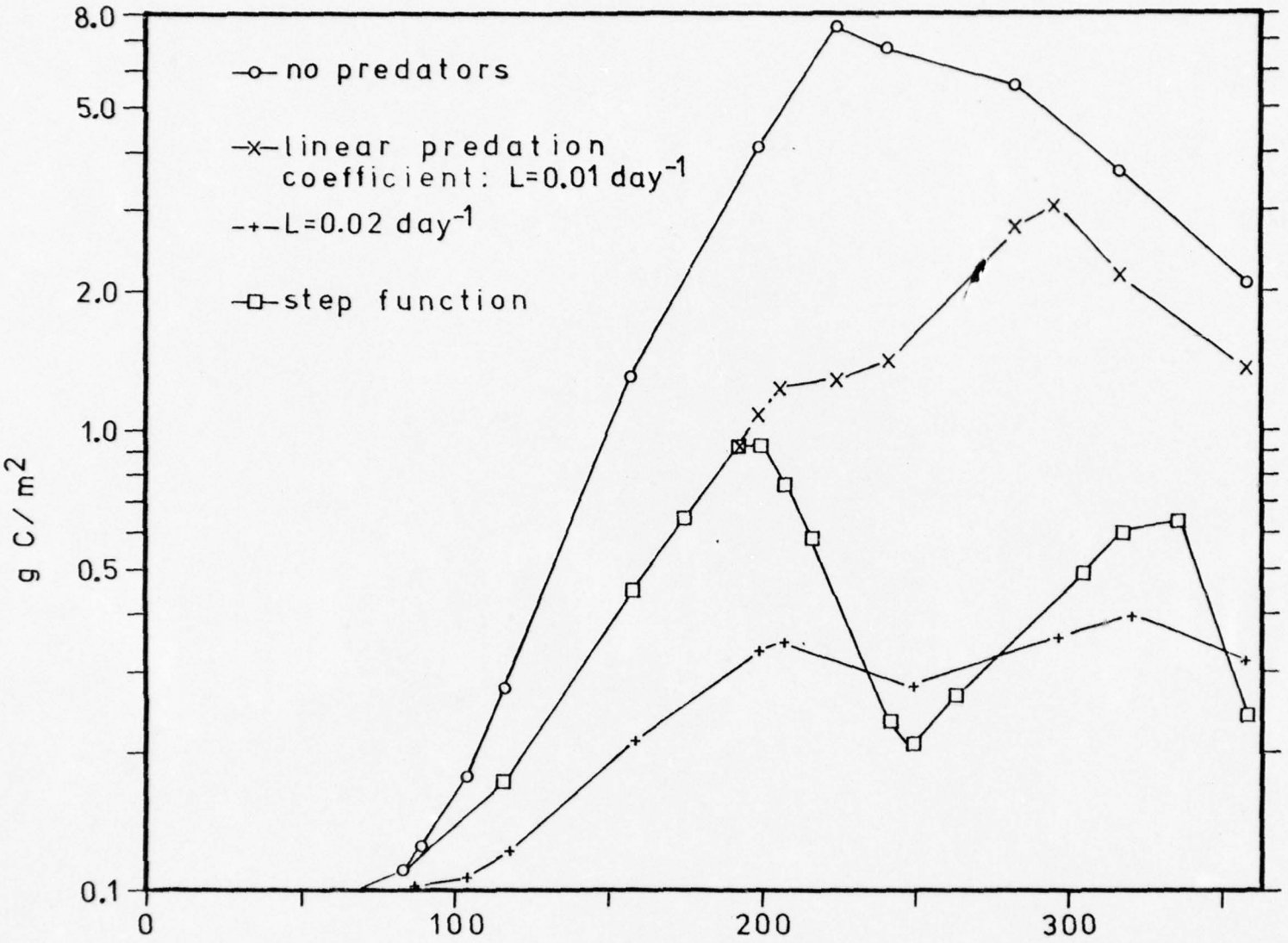

Figure 25. Simulated zooplankton response to various predation conditions (algal sinking rate = 1.0 m/day and advection coefficient = 0.1 m^{-1}).

C. COMPARISON OF SIMULATION RESULTS WITH OBSERVED DATA

The computer simulation was run with the new upwelling and radiation indices and the step function predation pressure term detailed in the preceding section. The sinking rate was set at 1.6 m/day and the advection coefficient set to $K = 0.1\ m^{-1}$.

A comparison of the simulation results with data observed by Traganza et al. (1976) is shown in Figures 26, 27, and 28. The calculated nutrient values lag the averaged mixed layer concentrations by 20 to 30 days during the summer months with a moderate amount of error in magnitude. The nutrient maximum occurs on day 144 with a value of 2.08 µg-at P/l in the simulation. A rapid decrease in phosphate levels coincident with the summer phytoplankton bloom displays the impact of nutrient uptake by phytoplankton in the model.

The simulated phytoplankton peak occurs 40 days after the nutrient peak during the period of maximum incident radiation (see Appendix C). The modeled response of phytoplankton was relatively inflexible with regard to the radiation index, i.e. the phytoplankton peak was found to occur within a few days of the time of maximum incident radiation when the sinking rate was varied from about 1.0 m/day to 1.8 m/day. The relationship of the phytoplankton peak to the radiation peak is explained by examination of the phytoplankton growth equations (shown in Appendix B). A slight increase in phytoplankton biomass was simulated during December (day 330) which could be due to the increased phosphate concentration at the end of the year.

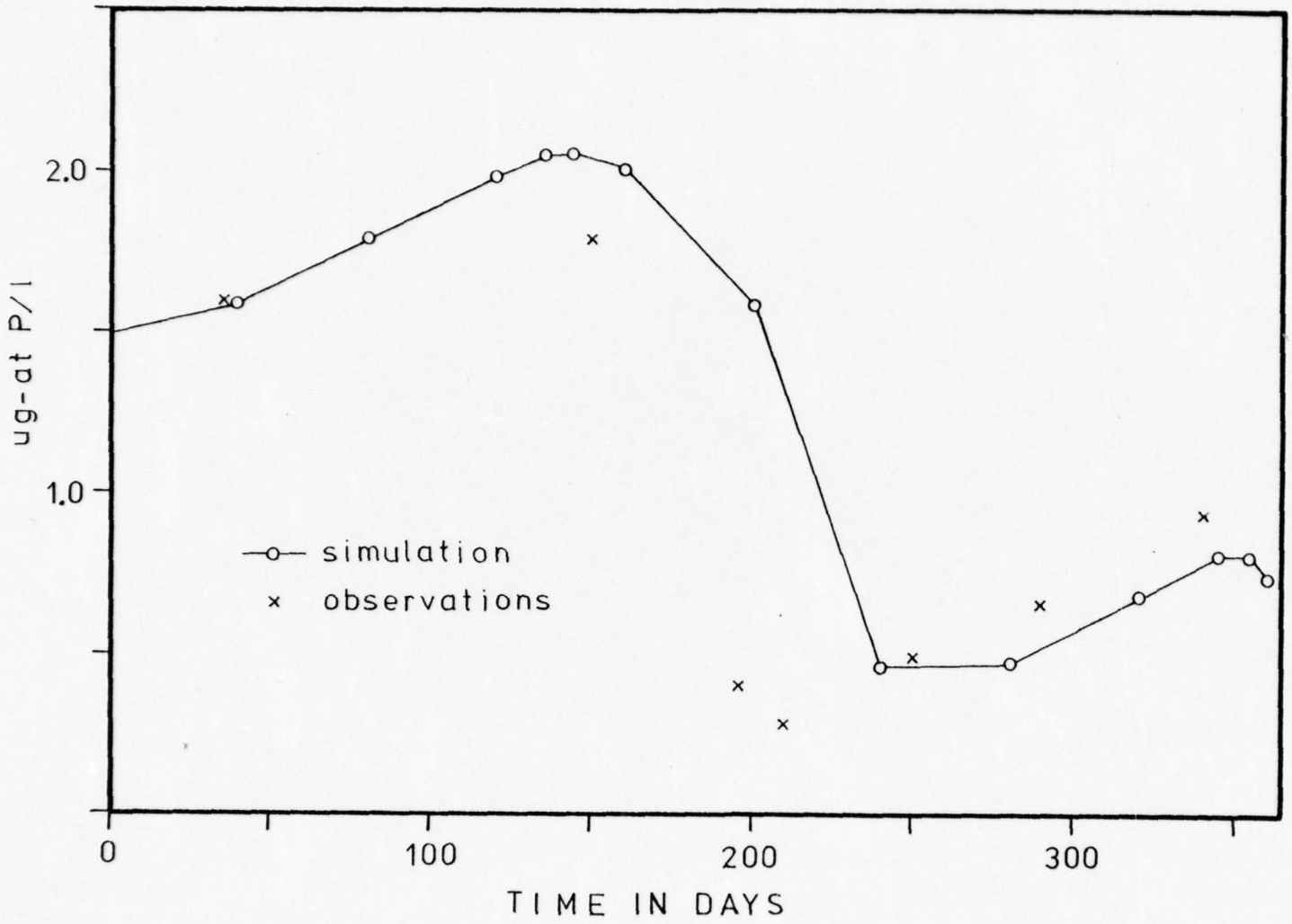

Figure 26. Comparison of simulated seasonal phosphate with observed data.

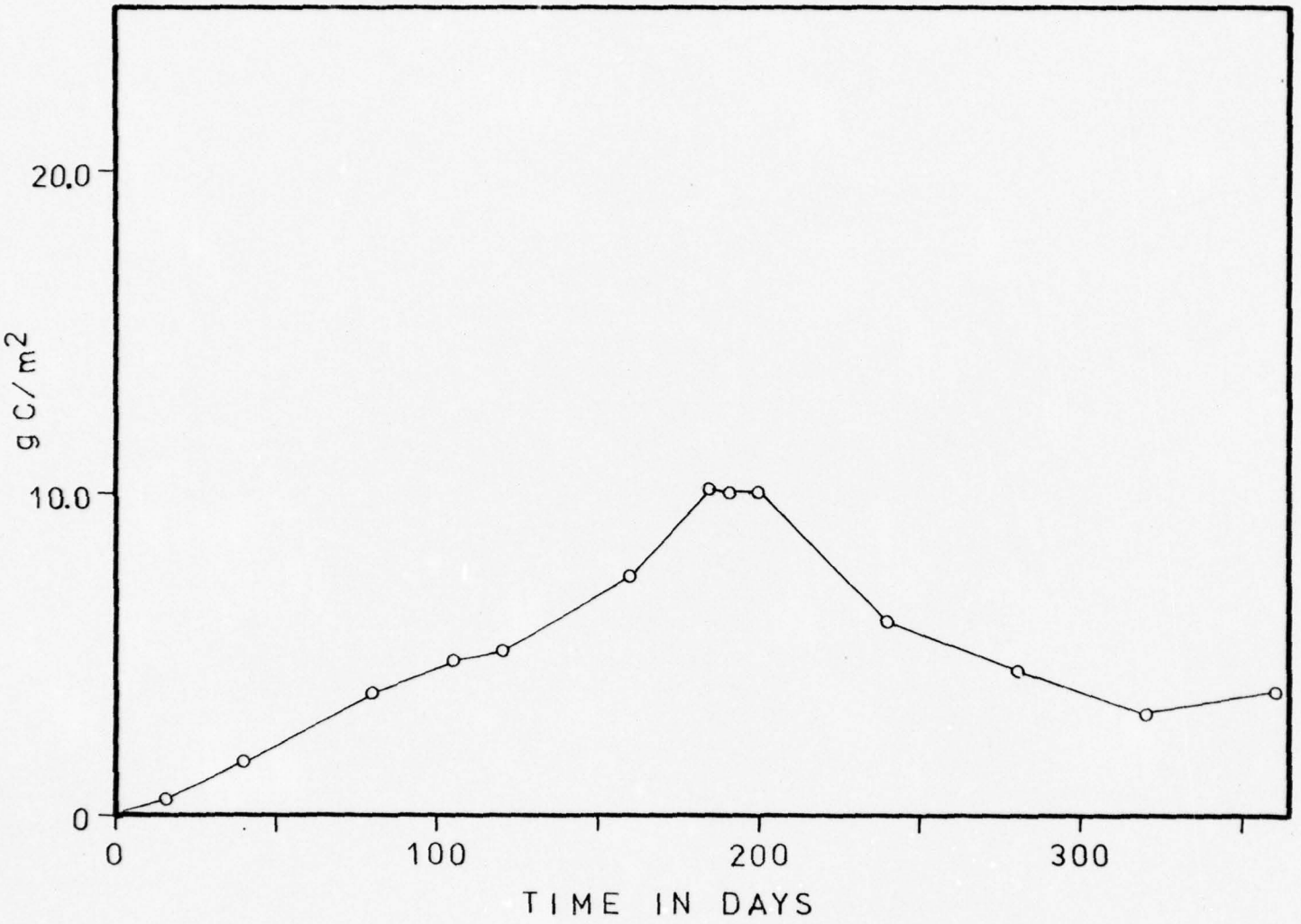

Figure 27. Simulated seasonal phytoplankton concentration.

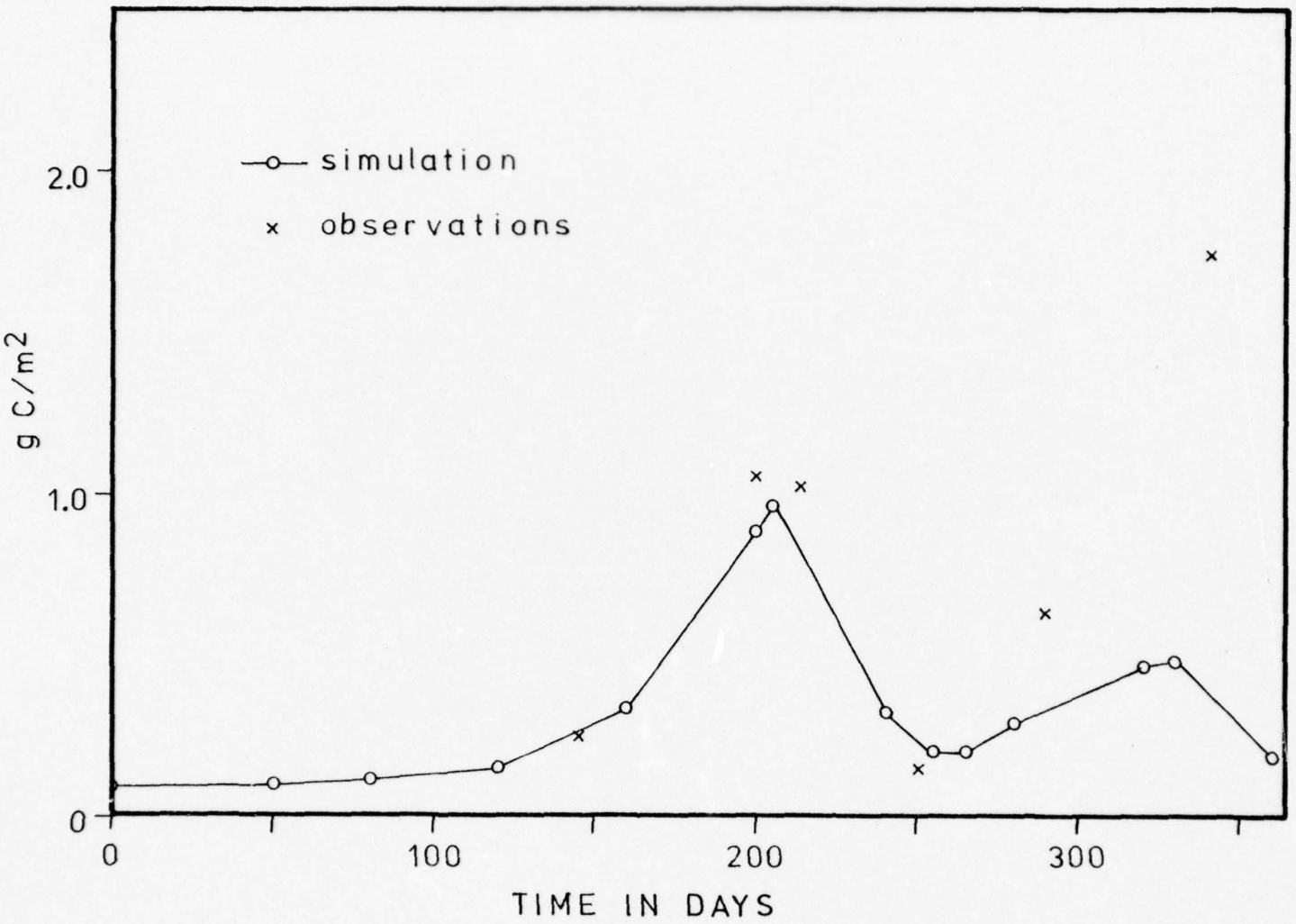

Figure 28. Comparison of simulated seasonal zooplankton concentration with observed data.

Twenty days after the phytoplankton maximum, the model simulated a zooplankton peak with a concentration of 0.97 g C/m^2. The zooplankton biomass growth corresponds well with the observed data until approximately the beginning of September. The measured values increase to a maximum of 1.85 g C/m^2 in mid-December while the model simulated a recovery peak of 0.47 g C/m^2 and slightly earlier.

V. DISCUSSION

The Monterey upwelling ecosystem simulation developed in this thesis has been shown to follow the seasonal trends of the observed phosphate, phytoplankton, and zooplankton data. There are errors in magnitude of the simulated response at various times of the year. The differences between observed and simulated zooplankton are most likely due to the fact that the model simulates herbivorous zooplankton while the observations include both herbivores and carnivores. Quantitative data defining the seasonal ratio of herbivorous to carnivorous zooplankton are needed to verify the simulation results. The encouraging aspect of the model is its ability to follow the seasonal trends and the fact that the timing of the response of phytoplankton biomass to the nutrient concentration and the response of zooplankton to the phytoplankton cycle is biologically sound, i.e. a moderate delay is simulated between the peaks of successive trophic levels.

Since all the factors likely to affect the three state variables (phosphate, phytoplankton and zooplankton) are not included in the model, some error in magnitude should appear. In recalling the philosophy expressed earlier, the objective of this thesis has been to create a time simulation of the dynamics of phosphate, phytoplankton and herbivorous zooplankton in a limited area over a long time. This objective

has been met by balancing the four model characteristics of generality, realism, precision and simplicity.

From studies by Barham (1957) and Bolin (1964) it is noted that there may be characteristic seasonal patterns of plankton dynamics in response to characteristic patterns of the hydrography of the Monterey upwelling ecosystem. It is perhaps important to realize that the apparent limitations of the model as developed thus far are relatively small when the use of the simulation to reproduce the characteristic patterns is considered *per se*.

As more and better data with which to define the dynamics are obtained, the simulation model of the Monterey upwelling ecosystem can progress to a more refined level.

VI. SUGGESTIONS FOR FURTHER RESEARCH

The following comments are made as a result of questions which arose during the modification of the Monterey ecosystem model. This list is provided to identify some areas which may warrant further investigation. It is by no means complete, but should serve as a guide.

1. The most significant outcome of this research has been the recognition of the importance of accurate forcing functions. The presence of the submarine canyon in Monterey Bay and the likely effect on upwelling suggests further effort be directed to verifying the upwelling index.

2. The Monterey Bay area is not homogeneous in physical, chemical and biological parameters as evidenced by the patchiness of biological samples and the observable spatial gradients of the physical and chemical properties.

3. Additional work on the biological aspects of the model including verification and refinement of the predation terms and development of an appropriate kinetic expression is indicated.

4. The simulation appears overly-sensitive to temperature variations in the mixed layer.

5. Various investigators have shown the importance of phytophagous fish in ecosystem models. A fish herbivore term should be investigated.

6. Some question as to the stability of the CSMP 360 routine over long time simulation has been raised. This might be investigated and resolved by initializing the model part way through the year.

7. The effect of varying the forcing functions in the revised model has not yet been studied.

8. The advection expression might be expanded to include the effects of all current systems influencing the Monterey region.

APPENDIX A: MONTEREY BAY UPWELLING PROGRAM

```
C ***********************************************************************
C ***********************************************************************
C ***********************************************************************
C ***********************************************************************
C ****                                                               *****
C ****                                                               *****
C ****    THE FOLLOWING PROGRAM IS USED TO CALCULATE THE ANNUAL      *****
C ****    CYCLE OF UPWELLING IN MONTEREY BAY, CALIFORNIA.  DAILY MEAN*****
C ****    WIND SPEED AND DIRECTION IS USED TO COMPUTE THE WIND STRESS *****
C ****    TAU, AT THE SEA SURFACE.  FROM EKMAN THEORY OF WIND DRIVEN  *****
C ****    CIRCULATION, THE NET OFFSHORE COMPONENT OF CURRENT IN THE   *****
C ****     MIXED LAYER IS DETERMINED.  THE UPWELLING VELOCITY IS THEN *****
C ****    CALCULATED USING PRINCIPLES OF MASS CONTINUITY.            *****
C ****                                                               *****
C ****                                                               *****
C ***********************************************************************
C ***********************************************************************
C ***********************************************************************
C ***********************************************************************
C
C
      DIMENSION DAY(370), WINDIR(370), WINSPD(370)
      DIMENSION WCOAST(370), CZ(370), TAU(370), VZERO(370), UBAR(370)
      DIMENSION W(370)
      DIMENSION UPWELL(370)
      DIMENSION XPORT(370)
      DIMENSION ARGMNT(370)
      DIMENSION MAXDIR(370)
      DIMENSION DATE(370)
      DIMENSION AVGUP(400),IDAY(400),ADAY(400),AUPWLL(400)
      DIMENSION VAR(400),AVG(400)
      DIMENSION XDAY(400)
      DIMENSION CORDIR(400)
      LOGICAL*1 NAME(80)/80*' '/
      INFILE=5
      IPRINT=6
      IMAX=365
      DO 8000 I=1,IMAX
C
C FIXED CONSTANTS ARE GIVEN:
C
      RHOWAT=1.02
      RHOAIR=0.00122
      A=100.0
      OMEGA=0.0000727
      COAST=330.0
```

```
      EKMAN=50.0
      WIDTH=30000.0
      ALAT=(36.75/180.0)*3.141592
      SINLAT=SIN(ALAT)
C WIND SPEED IS READ IN KNOTS, THEN CONVERTED TO METERS/SECOND.
      READ(INFILE,10)DATE(I),WINSPD(I),MAXDIR(I)
      DAY(I)=I
   10 FORMAT(I9,5X,F4.1,1X,I3)
C
C CORRECTIONS ARE APPLIED TO THE RAW WIND DATA.
C
      IF(MAXDIR(I).LE.240.AND.MAXDIR(I).GE.60)GO TO 20
      GO TO 21
   20 MAXDIR(I)=MAXDIR(I)+20
      WINSPD(I)=WINSPD(I)*1.5
      GO TO 22
   21 MAXDIR(I)=MAXDIR(I)+10
      WINSPD(I)=WINSPD(I)*1.1
   22 WINDIR(I)=MAXDIR(I)
C
C     THE VARIABLE 'CORDIR(I)' IS COMPUTED TO PRESENT THE POLAR PLOT
C     IN A GEOGRAPHIC ORIENTATION.
C
      CORDIR(I)=WINDIR(I)+(360.0-WINDIR(I))*2.0
      WINSPD(I)=WINSPD(I)*0.508
C
C WCOAST IS THE COMPONENT OF THE WIND VECTOR BLOWING PARALLEL TO
C THE COAST.  CALIFORNIA COAST IN THIS REGION IS ORIENTED 150-330 DEG.
C
      ARGMNT(I)=(((WINDIR(I)-COAST)/360.0)*6.283)
      WCOAST(I)=WINSPD(I)*COS(ARGMNT(I))
      W(I)=WCOAST(I)
C
C THE DRAG COEFFICIENT IS FIRST CALCULATED AS A FUNCTION OF THE WIND
C SPEED BY DEACON'S RELATIONSHIP: 0.001(1.1+0.04W)
C
      IF(WCOAST(I).LE.0.0)W(I)=W(I)*(-1.0)
      CZ(I)=(1.10+0.04*W(I))*0.001
C
C THE WIND STRESS, TAU, IS THEN CALCULATED.
C
      TAU(I)=RHOAIR*CZ(I)*((W(I)*100.0)**2)
      IF(WCOAST(I).LE.0.0)TAU(I)=TAU(I)*(-1.0)
C
C THE SURFACE CURRENT VECTOR, VZERO, IS THEN FOUND.  VZERO LIES 45
C DEGREES TO THE RIGHT OF THE WIND
C NEGATIVE VALUES OF CURRENT AND TRANSPORT INDICATE ONSHORE FLOW AND
C CONVERGENCE WITH SUBSEQUENT DOWNWELLING.
```

```
C
      VZERO(I)=TAU(I)/(A*((2.0*OMEGA*SINLAT*RHOWAT/A)**0.5))
C
C THE AVERAGE HORIZONTAL CURRENT COMPONENT IN THE EKMAN LAYER, D, IS
C CALCULATED BY EVALUATING THE INTEGRAL  OF UDZ OVER THE RANGE OF
C DEPTH ZERO TO D.
C
      UBAR(I)=0.225079*VZERO(I)
C
C VALUES OF OFFSHORE TRANSPORT, XPORT, ARE GIVEN IN KG/CM/SEC.
C
      XPORT(I)=TAU(I)/(2.0*OMEGA*SINLAT)
C
C THE VERTICAL VELOCITY RESULTING FROM THE TRANSPORT OF WATER OFFSHORE
C BY THE HORIZONTAL COMPONENT, UBAR, IS DETERMINED BY USING PRINCIPALS
C OF MASS CONSERVATION WITHIN A VOLUME OF WATER REPRESENTING THE UPWELLING
C REGION.
C VALUES OF UPWELL ARE CONVERTED TO METERS/DAY.
C
      UPWELL(I)=(UBAR(I)*(EKMAN/WIDTH))*(86400.0/100.0)
 8000 CONTINUE
      JF=30
      NSIZE=365/JF
      N=1
      DO 999 J=1,NSIZE
      M=N+JF-1
      SUM=0.0
      DO 888 I=N,M
      SUM=SUM+UPWELL(I)
  888 CONTINUE
      AVG(J)=SUM/JF
      XDAY(J)=N+((JF/2)-1)
      N=M+1
  999 CONTINUE
      CALL CRVFIT(1,12,XDAY,AVG,6,67,ADAY,AUPWLL)
      WRITE(IPRINT,70)
   70 FORMAT(1H1)
      WRITE(IPRINT,80)
   80 FORMAT(1X,15HYR/MO/DA/JULIAN,3X,4HWIND,8X,4HWIND,4X,7HSURFACE,
     13X,7HAVERAGE,3X,9HUPWELLING)
      WRITE(IPRINT,81)
   81 FORMAT(19X,9HDIRECTION,3X,5HSPEED,3X,7HCURRENT,3X,7HCURRENT,3X,
     18HVELOCITY)
      WRITE(IPRINT,90)
   90 FORMAT(19X,8HDEG TRUE,4X,5HM/SEC,3X,6HCM/SEC,4X,6HCM/SEC,4X,
     15HM/DAY)
      WRITE(IPRINT,82)
   82 FORMAT(1HO)
```

```
      DO 8060 I=1,IMAX
      WRITE(IPRINT,83)DATE(I),WINDIR(I),WINSPD(I),VZERO(I),UBAR(I),
     1UPWELL(I)
   83 FORMAT(1X,I9,9X,F5.1,7X,F4.1,4X,F8.4,3X,F8.4,3X,F8.4)
 8060 CONTINUE
      WRITE(IPRINT,19)
   19 FORMAT(1H1)
      WRITE(IPRINT,15)
   15 FORMAT(2X,'THE AVERAGED VALUES OF DAYS AND UPWELL ARE:')
      WRITE(IPRINT,17)
   17 FORMAT(1H0)
      WRITE(IPRINT,16)
   16 FORMAT(2X,'DAY',20X,'UPWELLING VELOCITY')
      WRITE(IPRINT,18)
   18 FORMAT(1H0)
      DO 12 J=1,67
      WRITE(IPRINT,11)ADAY(J),AUPWLL(J)
   11 FORMAT(2X,F5.1,18X,F9.5)
   12 CONTINUE
      WRITE(IPRINT,6001)
 6001 FORMAT(1H1)
      CALL PLOTP(XDAY(1),AVG(1),NSIZE,0)
      WRITE(IPRINT,6000)
 6000 FORMAT(1H1)
      CALL PLOTP(ADAY(1),AUPWLL(1),67,0)
      WRITE(IPRINT,6002)
 6002 FORMAT(1H1)
      CALL POLEPR(2,NAME(1),IMAX,CORDIR(1),WINSPD(1),10.0)
   40 STOP
      END
```

APPENDIX B: MONTEREY BAY ECOSYSTEM MODEL PROGRAM

```
TITLE    MONTEREY UPWELLING ECOSYSTEM
************************************************************************
** THIS MODEL SIMULATES THE SEASONAL FLUCTUATIONS IN THREE STATE      **
** VARIABLES- MIXED LAYER PHOSPHATE CONCENTRATION (X1), PHYTOPLANKTON **
** BIOMASS (X2), AND HERBIVOROUS ZOOPLANKTON BIOMASS (X3). THE        **
** SIMULATION RESULTS ARE DEPENDENT ON ANNUAL VARIATIONS IN FOUR      **
** ENVIRONMENTAL PARAMETERS THAT INFLUENCE BIOLOGICAL PRODUCTIVITY    **
** IN A REGION OF UPWELLING.  THE PARAMETERS INCLUDE INCIDENT RADI-   **
** ATION (RADI), UPWELLING VELOCITY (W), MIXED LAYER TEMPERATURE      **
** (TEMP), AND MIXED LAYER DEPTH (Z).                                 **
************************************************************************
************************************************************************
INITIAL
      INCON IC1=1.5, IC2=0.1, IC3=0.1
      CONSTANT B=0.5, C=0.774, DX1=3.0, FKL=50.0, FAVL=0.8, KG=80.0,...
      KN=0.6, L=0.01, M=0.12, MAXG=0.25, P=2.5, R=0.069,...
      RHOZ2=0.0175, RHOZ3=0.019, S=0.13, X1MIN=0.0, X2MIN=16.0,...
      WFAC=0.6, ZFAC=1.0, TFAC=1.0, RFAC=1.0, V=1.0
DYNAMIC
************************************************************************
** ENVIRONMENTAL FUNCTIONS ARE DEFINED BY THE LINEAR FUNCTION        **
** GENERATOR, AFGEN.                                                **
************************************************************************
************************************************************************
**      THE SOLAR FUNCTION IS DERIVED FROM TONT'S METHOD            **
************************************************************************
      FUNCTION SOLAR=(00.,.175),(30.,.189),(60.,.235),...
      (90.,.281),(120.,.296),(150.,.335),(180.,.406),...
      (210.,.364),(240.,.345),(270.,.303),(300.,.242),...
      (330.,.195),(360.,.185),(365.,.175)
      RCOMP=AFGEN(SOLAR,TIME)
************************************************************************
**      THE FOLLOWING UPWELL FUNCTION IS DERIVED FROM THE MEAN DAILY **
**      WINDS OVER MONTEREY BAY.                                    **
************************************************************************
      FUNCTION UPWELL=(0.,-.14),(15.,.05),(45.,.20),(75.,.39),...
      (105.,.73),(135.,1.),(165.,.57),(195.,.62),...
      (225.,.45),(260.,.36),(290.,.15),(315.,.35),...
      (345.,-.004),(365.,-.51)
      WCOMP=AFGEN(UPWELL,TIME)
      FUNCTION STEMP=(0.,12.0),(51.,10.8),(150.,11.4),(204.,12.7),...
      (217.,15.8),(253.,13.5),(297.,15.1),(344.,13.1),(365.,12.0)
      TCOMP=AFGEN(STEMP,TIME)
      FUNCTION LAYER=(0.,70.),(51.,100.),(150.,47.),(204.,33.),...
      (217.,13.),(253.,20.),(297.,24.),(344.,65.),(365.,70.)
      ZCOMP=AFGEN(LAYER,TIME)
************************************************************************
** VARIATIONS IN ENVIRONMENTAL PARAMETERS ARE GENERATED BY            **
```

```
** MULTIPLYING THE COMPUTED VALUE BY A CONSTANT FACTOR, I.E., WFAC    **
** ZFAC, ETC.                                                         **
**********************************************************************
      RADI=RFAC*RCOMP
      W=WFAC*WCOMP
      TEMP=TFAC*TCOMP
      Z=ZFAC*ZCOMP
**********************************************************************
** NEXT, VARIABLES REQUIRED IN RATE EQUATIONS ARE CALCULATED.        **
**********************************************************************
      MAXN=S*TEMP+B
      NTLIM=MAXN*(X1-X1MIN)/(KN+(X1-X1MIN))
      CL=33.333*(X2/Z)
      K=0.04+0.0088*CL+0.05*CL**0.666666
      X2MG=1000.*(X2/Z)
      UPWEL=(W/EKL)*(DX1-X1)
      MIX=(M/Z)*(DX1-X1)
      RAD=RADI/(K*Z)*(1.0-EXP(-K*Z))
**********************************************************************
** RATE EQUATIONS ARE COMPUTED.                                      **
**********************************************************************
      TAU12=P*RAD*NTLIM
      TAU23=MAXG*(X2MG-X2MIN)/(KG+(X2MG-XIMIN))
      NOSORT
      IF(TAU23.LT.0.0) TAU23=0.0
**********************************************************************
** THE PREDATOR POPULATION IS GOVERNED BY THE CONDITIONS:            **
**********************************************************************
      IF(X3DOT.GT.0.AND.X3.LT.1.0)FISH=1.0
      IF(X3DOT.GT.0.AND.X3.GE.1.0)FISH=5.0
      IF(X3DOT.LE.0.AND.X3.GE.0.2)FISH=5.0
      IF(X3DOT.LE.0.AND.X3.LT.0.2)FISH=1.0
      SORT
      TAU30=(0.8*(TAU23/MAXG))*TAU23
      TAU31=FAVL*(C/Z)*TAU30
      RHO20=RHOZ2*EXP(R*TEMP)
      RHO30=RHOZ3*EXP(R*TEMP)
      LAM02=W/Z
      LAM20=V/Z
      LAM30=L*FISH
**********************************************************************
** FLUXES ARE COMPUTED FROM RATE EQUATIONS.                          **
**********************************************************************
      NUT=UPWEL+MIX
      REGEN=TAU31*X3
      UPTAK=C*TAU12*(X2/Z)
      PROD=TAU12*X2
      RESP2=RHO20*X2
```

```
      GRAZ=TAU23*X3
      SINK=(LAM20-LAM02)*X2
      ADVEC2=W*X2*0.1
      RESP3=RH030*X3
      VOID=TAU30*X3
      LOSS=LAM30*X3
*************************************************************
** CHANGES IN THE STATE VARIABLES ARE COMPUTED AS THE SUM OF FLUXES.  **
*************************************************************
      X1DOT=NUT+REGEN-UPTAK
      X2DOT=PROD-RESP2-GRAZ-SINK-ADVEC2
      X3DOT=GRAZ-RESP3-VOID-LOSS
      X3DOT2=DERIV(0.0,X3DOT)
*************************************************************
** FINALLY, THE NEW VALUES FOR THE STATE VARIABLES ARE COMPUTED.      **
*************************************************************
      X1=INTGRL(IC1,X1DOT)
      X2=INTGRL(IC2,X2DOT)
      X3=INTGRL(IC3,X3DOT)
      NOSORT
      IF(X3.LT.0.1) X3=0.1
      TIMER FINTIM=365.0, OUTDEL=8.0
      PRTPLOT RCOMP
      PRTPLOT WCOMP
      PRTPLOT TCOMP
      PRTPLOT ZCOMP
      PRTPLOT FISH
      PRTPLOT X1(NUT, REGEN, UPTAK)
      PRTPLOT ADVEC2
      PRTPLOT X2(PROD, RESP2, GRAZ)
      PRTPLOT X3(GRAZ, RESP3, VOID)
      PRTPLOT X3DOT2
      END
      STOP
ENDJOB
```

APPENDIX C: FORCING FUNCTIONS USED IN SIMULATION

MIXED LAYER DEPTH
(ZCOMP) VERSUS TIME

MINIMUM 1.3243E 01 — MAXIMUM 1.0000E 02

TIME	ZCOMP
0.0	7.0000E 01
8.0000E 00	7.4706E 01
1.6000E 01	7.9412E 01
2.4000E 01	8.4118E 01
3.2000E 01	8.8824E 01
4.0000E 01	9.3529E 01
4.8000E 01	9.8235E 01
5.6000E 01	9.7323E 01
6.4000E 01	9.3040E 01
7.2000E 01	8.8758E 01
8.0000E 01	8.4475E 01
8.8000E 01	8.0192E 01
9.6000E 01	7.5909E 01
1.0400E 02	7.1626E 01
1.1200E 02	6.7343E 01
1.2000E 02	6.3061E 01
1.2800E 02	5.8778E 01
1.3600E 02	5.4495E 01
1.4400E 02	5.0212E 01
1.5200E 02	4.6481E 01
1.6000E 02	4.4407E 01
1.6800E 02	4.2333E 01
1.7600E 02	4.0259E 01
1.8400E 02	3.8185E 01
1.9200E 02	3.6111E 01
2.0000E 02	3.4037E 01
2.0800E 02	2.6846E 01
2.1600E 02	1.4538E 01
2.2400E 02	1.4361E 01
2.3200E 02	1.5917E 01
2.4000E 02	1.7472E 01
2.4800E 02	1.9028E 01
2.5600E 02	2.0273E 01
2.6400E 02	2.1000E 01
2.7200E 02	2.1727E 01
2.8000E 02	2.2455E 01
2.8800E 02	2.3182E 01
2.9600E 02	2.3909E 01
3.0400E 02	3.0106E 01
3.1200E 02	3.7085E 01
3.2000E 02	4.4064E 01
3.2800E 02	5.1043E 01
3.3600E 02	5.8021E 01
3.4400E 02	6.5000E 01
3.5200E 02	6.6905E 01
3.6000E 02	6.8810E 01

INCIDENT RADIATION

(RCOMP) VERSUS TIME

MINIMUM 1.7500E-01 — MAXIMUM 4.0600E-01

TIME	RCOMP
0.0	1.7500E-01
8.0000E 00	1.7873E-01
1.6000E 01	1.8247E-01
2.4000E 01	1.8620E-01
3.2000E 01	1.9207E-01
4.0000E 01	2.0433E-01
4.8000E 01	2.1660E-01
5.6000E 01	2.2887E-01
6.4000E 01	2.4113E-01
7.2000E 01	2.5340E-01
8.0000E 01	2.6567E-01
8.8000E 01	2.7793E-01
9.6000E 01	2.8400E-01
1.0400E 02	2.8800E-01
1.1200E 02	2.9200E-01
1.2000E 02	2.9600E-01
1.2800E 02	3.0640E-01
1.3600E 02	3.1680E-01
1.4400E 02	3.2720E-01
1.5200E 02	3.3973E-01
1.6000E 02	3.5867E-01
1.6800E 02	3.7760E-01
1.7600E 02	3.9653E-01
1.8400E 02	4.0040E-01
1.9200E 02	3.8920E-01
2.0000E 02	3.7800E-01
2.0800E 02	3.6680E-01
2.1600E 02	3.6020E-01
2.2400E 02	3.5513E-01
2.3200E 02	3.5007E-01
2.4000E 02	3.4500E-01
2.4800E 02	3.3380E-01
2.5600E 02	3.2260E-01
2.6400E 02	3.1140E-01
2.7200E 02	2.9893E-01
2.8000E 02	2.8267E-01
2.8800E 02	2.6640E-01
2.9600E 02	2.5013E-01
3.0400E 02	2.3573E-01
3.1200E 02	2.2320E-01
3.2000E 02	2.1067E-01
3.2800E 02	1.9813E-01
3.3600E 02	1.9300E-01
3.4400E 02	1.9033E-01
3.5200E 02	1.8767E-01
3.6000E 02	1.8500E-01

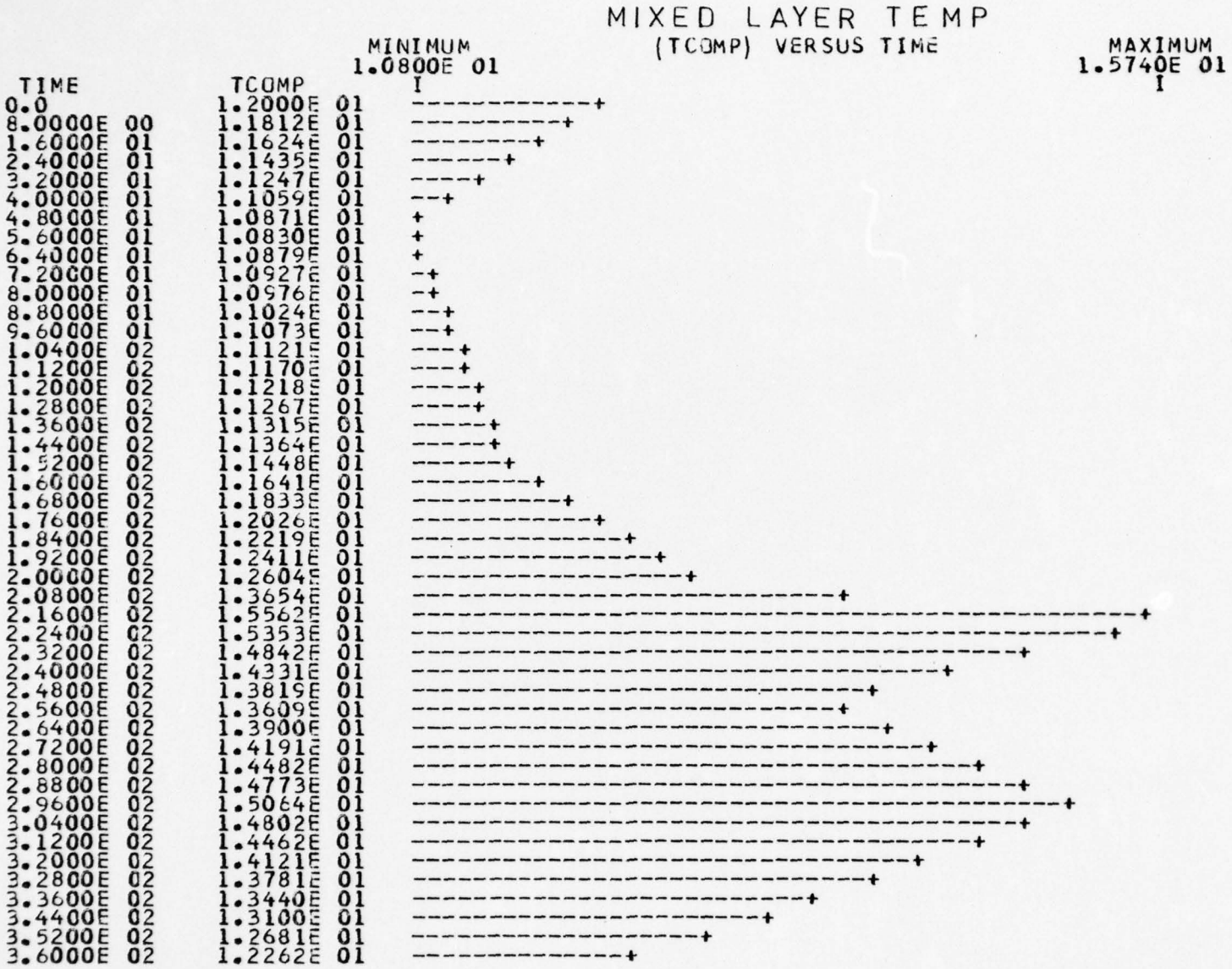
MIXED LAYER TEMP
(TCOMP) VERSUS TIME
MINIMUM
1.0800E 01
MAXIMUM
1.5740E 01
TIME
TCOMP
0.0 1.2000E 01
8.0000E 00 1.1812E 01
1.6000E 01 1.1624E 01
2.4000E 01 1.1435E 01
3.2000E 01 1.1247E 01
4.0000E 01 1.1059E 01
4.8000E 01 1.0871E 01
5.6000E 01 1.0830E 01
6.4000E 01 1.0879E 01
7.2000E 01 1.0927E 01
8.0000E 01 1.0976E 01
8.8000E 01 1.1024E 01
9.6000E 01 1.1073E 01
1.0400E 02 1.1121E 01
1.1200E 02 1.1170E 01
1.2000E 02 1.1218E 01
1.2800E 02 1.1267E 01
1.3600E 02 1.1315E 01
1.4400E 02 1.1364E 01
1.5200E 02 1.1448E 01
1.6000E 02 1.1641E 01
1.6800E 02 1.1833E 01
1.7600E 02 1.2026E 01
1.8400E 02 1.2219E 01
1.9200E 02 1.2411E 01
2.0000E 02 1.2604E 01
2.0800E 02 1.3654E 01
2.1600E 02 1.5562E 01
2.2400E 02 1.5353E 01
2.3200E 02 1.4842E 01
2.4000E 02 1.4331E 01
2.4800E 02 1.3819E 01
2.5600E 02 1.3609E 01
2.6400E 02 1.3900E 01
2.7200E 02 1.4191E 01
2.8000E 02 1.4482E 01
2.8800E 02 1.4773E 01
2.9600E 02 1.5064E 01
3.0400E 02 1.4802E 01
3.1200E 02 1.4462E 01
3.2000E 02 1.4121E 01
3.2800E 02 1.3781E 01
3.3600E 02 1.3440E 01
3.4400E 02 1.3100E 01
3.5200E 02 1.2681E 01
3.6000E 02 1.2262E 01

UPWELLING INDEX

(WCOMP) VERSUS TIME

MINIMUM -3.8350E-01 I

MAXIMUM 9.9100E-01 I

TIME	WCOMP
0.0	-1.4000E-01
8.0000E 00	-3.8667E-02
1.6000E 01	5.5000E-02
2.4000E 01	9.5000E-02
3.2000E 01	1.3500E-01
4.0000E 01	1.7500E-01
4.8000E 01	2.1900E-01
5.6000E 01	2.6967E-01
6.4000E 01	3.2033E-01
7.2000E 01	3.7100E-01
8.0000E 01	4.4667E-01
8.8000E 01	5.3733E-01
9.6000E 01	6.2800E-01
1.0400E 02	7.1867E-01
1.1200E 02	7.9300E-01
1.2000E 02	8.6500E-01
1.2800E 02	9.3700E-01
1.3600E 02	9.8567E-01
1.4400E 02	8.7100E-01
1.5200E 02	7.5633E-01
1.6000E 02	6.4167E-01
1.6800E 02	5.7500E-01
1.7600E 02	5.6833E-01
1.8400E 02	6.0167E-01
1.9200E 02	6.1500E-01
2.0000E 02	5.9167E-01
2.0800E 02	5.4633E-01
2.1600E 02	5.0100E-01
2.2400E 02	4.5567E-01
2.3200E 02	4.3200E-01
2.4000E 02	4.1143E-01
2.4800E 02	3.9086E-01
2.5600E 02	3.7029E-01
2.6400E 02	3.3200E-01
2.7200E 02	2.7600E-01
2.8000E 02	2.2000E-01
2.8800E 02	1.6400E-01
2.9600E 02	1.9800E-01
3.0400E 02	2.6200E-01
3.1200E 02	3.2600E-01
3.2000E 02	2.9100E-01
3.2800E 02	1.9660E-01
3.3600E 02	1.0220E-01
3.4400E 02	7.8001E-03
3.5200E 02	-1.8110E-01
3.6000E 02	-3.8350E-01

LIST OF REFERENCES

1. Bakun, A., Coastal Upwelling Indices, West Coast of North America, 1946-1971, NOAA Technical Report NNFS SSRF-671, 1973.

2. Bannister, T. T., "A General Theory of Steady State Phytoplankton Growth in a Nutrient Saturated Mixed Layer," Limnology and Oceanography, v. 19(1) pp. 13-30, January 1974.

3. Barham, E. G., The Ecology of Sonic Scattering Layers in the Monterey Bay Area, Hopkins Marine Station, Stanford University, California, February 11, 1957.

4. Bolin, R. L., Hydrographic Data from the Area of the Monterey Submarine Canyon, 1951-1955, Hopkins Marine Station, Stanford University, California, 1964.

5. Bolin, R. L. and D. P. Abbott, "Studies on the Marine Climate of the Central Coastal Area of California, 1954-1960," California Cooperative Fisheries Investigation Reports, v. 9, pp. 23-45, 1962.

6. California Cooperative Fisheries Investigation (CALCOFI), Atlas Number 20, State of California Marine Resources Committee, June 1974.

7. Gordon, A. L., Studies in Physical Oceanography, Gordon and Breach, 1972.

8. Lehman, J. T., D. B. Botkin, and G. E. Likens, "The Assumptions and Rationales of a Computer Model of Phytoplankton Population Dynamics," Limnology and Oceanography, v. 20, pp. 343-364, May 1975.

9. Neumann, G., Ocean Currents, Elsevier Scientific Publishing Company, 1968.

10. Neumann, G. and W. J. Pierson, Principles of Physical Oceanography, Prentice-Hall Inc., Englewood Cliffs, New Jersey, 1966.

11. NOAA, The Environment of the United States Living Marine Resources 1974, MARMAP, January, 1976.

12. O'Brien, J. and J. S. Wrobleski, "On Advection in Phytoplankton Models," prepared for the Office of Naval Research, National Science Foundation, 1972.

13. Odum, E. P., Fundamentals of Ecology, W. B. Saunders Company, 1971.

14. Parsons, T. R. and M. Takahashi, Biological Oceanographic Processes, Pergammon Press, 1973.

15. Patten, B. C., Systems Analysis and Simulation in Ecology, V. I, Academic Press, 1971.

16. Pearson, R. T., A Computer Simulation Model of Seasonal Variations in Ocean Production for a Region of Upwelling, MS Thesis, Naval Postgraduate School, Monterey, California, 1975.

17. Roll, H. U., Physics of the Marine Atmosphere, Academic Press, 1965.

18. Smith, R. L., "Upwelling," 1968, in Oceanography and Marine Biology, edited by Barnes, H., pp. 11-46, 1969.

19. Sverdrup, H. U., M. W. Johnson, and R. H. Flemming, The Oceans, Their Physics, Chemistry and General Biology, Prentice-Hall, Inc., 1942.

20. Tont, S. A., "The Effect of Upwelling on Solar Irradiance Near the Coast of Southern California," Journal of Geophysical Research, v. 80, pp. 5031-5034, December 20, 1975.

21. Traganza. E. D., K. J. Graham, R. T. Pearson, J. C. Radney and J. S. Anderson. Carbon/Adenosine Triphosphate Ratios in Marine Zooplankton and the Annual Oceanography Off Monterey, California, 1974. Technical Report NPS-58Tg76041. Naval Postgraduate School, Monterey, California, 1976.

22. Walsh, J. J., Modelled Processes in the Sea, University of Washington, unpublished preprint, 1973.

23. Wilson, B. W., "Note on Surface Wind Stress over Water at Low and High Wind Speeds," Journal of Geophysical Research, v. 65(10), pp. 3377-3382, October 1960.

INITIAL DISTRIBUTION LIST

		No. Copies
1.	Department of Oceanography, Code 68 Naval Postgraduate School Monterey, California 93940	3
2.	Oceanographer of the Navy Hoffman Building No. 2 200 Stovall Street Alexandria, Virginia 22332	1
3.	Office of Naval Research Code 480 Arlington, Virginia 22217	1
4.	Dr. Robert E. Stevenson Scientific Liaison Office, ONR Scripps Institution of Oceanography La Jolla, California 92037	1
5.	Library, Code 3330 Naval Oceanographic Office Washington, D. C. 20373	1
6.	SIO Library University of California, San Diego P. O. Box 2367 La Jolla, California 92037	1
7.	Department of Oceanography Library University of Washington Seattle, Washington 98105	1
8.	Department of Oceanography Library Oregon State University Corvallis, Oregon 97331	1
9.	Commanding Officer Fleet Numerical Weather Central Monterey, California 93940	1
10.	Commanding Officer Navy Environmental Prediction Research Facility Monterey, California 93940	1

11.	Department of the Navy Commander Oceanographic System Pacific Box 1390 FPO San Francisco 96610	1
12.	Defense Documentation Center Cameron Station Alexandria, Virginia 22314	2
13.	Library (Code 0142) Naval Postgraduate School Monterey, California 93940	2
14.	Commander Naval Weather Service Command Washington Navy Yard Washington, D. C. 20390	1
15.	Commandant (G-PTE-1/72) U. S. Coast Guard Washington, D. C. 20591	2
16.	Department of Oceanography U. S. Coast Guard Academy New London, Connecticut 06320	2
17.	Dr. E. D. Traganza Department of Oceanography Naval Postgraduate School Monterey, California 93940	3
18.	Huseyin Yuce Dz. YZB Deniz Harbokulu Heybeliada/Istanbul Turkey	1
19.	LT D. E. Henrickson Marine Sciences Branch Commandant (G-000) U. S. Coast Guard Washington, D. C. 20591	2
20.	Dr. Glenn H. Jung Department of Oceanography Naval Postgraduate School Monterey, California 93940	1
21.	LCDR A. B. Chace Department of Oceanography Naval Postgraduate School Monterey, California 93940	1